



# Sea-ice melt CO<sub>2</sub>–carbonate chemistry in the western Arctic Ocean: meltwater contributions to air–sea CO<sub>2</sub> gas exchange, mixed-layer properties and rates of net community production under sea ice

N. R. Bates<sup>1</sup>, R. Garley<sup>1</sup>, K. E. Frey<sup>2</sup>, K. L. Shake<sup>2</sup>, and J. T. Mathis<sup>3,4</sup>

<sup>1</sup>Bermuda Institute of Ocean Sciences, St. Georges, Bermuda

<sup>2</sup>Graduate School of Geography, Clark University, 950 Main Street, Worcester, MA 01610, USA

<sup>3</sup>National Oceanic and Atmospheric Administration, Pacific Marine Environmental Lab, Seattle, WA, USA

<sup>4</sup>Ocean Acidification Research Center, University of Alaska Fairbanks, Fairbanks, AK, USA

Correspondence to: N. R. Bates (nick.bates@bios.edu)

Received: 3 December 2013 – Published in Biogeosciences Discuss.: 16 January 2014

Revised: 3 October 2014 – Accepted: 27 October 2014 – Published: 8 December 2014

**Abstract.** The carbon dioxide (CO<sub>2</sub>)-carbonate chemistry of sea-ice melt and co-located, contemporaneous seawater has rarely been studied in sea-ice-covered oceans. Here, we describe the CO<sub>2</sub>–carbonate chemistry of sea-ice melt (both above sea-ice as “melt ponds” and below sea-ice as “interface waters”) and mixed-layer properties in the western Arctic Ocean in the early summer of 2010 and 2011. At 19 stations, the salinity ( $\sim 0.5$  to  $< 6.5$ ), dissolved inorganic carbon (DIC;  $\sim 20$  to  $< 550 \mu\text{mol kg}^{-1}$ ) and total alkalinity (TA;  $\sim 30$  to  $< 500 \mu\text{mol kg}^{-1}$ ) of above-ice melt pond water was low compared to the co-located underlying mixed layer. The partial pressure of CO<sub>2</sub> ( $p\text{CO}_2$ ) in these melt ponds was highly variable ( $\sim < 10$  to  $> 1500 \mu\text{atm}$ ) with the majority of melt ponds acting as potentially strong sources of CO<sub>2</sub> to the atmosphere. The pH of melt pond waters was also highly variable ranging from mildly acidic (6.1 to 7) to slightly more alkaline than underlying seawater ( $> 8.2$  to 10.8). All of the observed melt ponds had very low ( $< 0.1$ ) saturation states ( $\Omega$ ) for calcium carbonate (CaCO<sub>3</sub>) minerals such as aragonite ( $\Omega_{\text{aragonite}}$ ). Our data suggest that sea-ice generated alkaline or acidic type melt pond water. This melt water chemistry dictates whether the ponds are sources of CO<sub>2</sub> to the atmosphere or CO<sub>2</sub> sinks. Below-ice interface water CO<sub>2</sub>–carbonate chemistry data also indicated substantial generation of alkalinity, presumably owing to dissolution of CaCO<sub>3</sub> in sea-ice. The interface waters generally had lower  $p\text{CO}_2$  and higher pH /  $\Omega_{\text{aragonite}}$  than the co-located mixed layer beneath. Sea-ice melt thus contributed to the suppression of

mixed-layer  $p\text{CO}_2$ , thereby enhancing the surface ocean’s capacity to uptake CO<sub>2</sub> from the atmosphere. Our observations contribute to growing evidence that sea-ice CO<sub>2</sub>–carbonate chemistry is highly variable and its contribution to the complex factors that influence the balance of CO<sub>2</sub> sinks and sources (and thereby ocean acidification) is difficult to predict in an era of rapid warming and sea-ice loss in the Arctic Ocean.

## 1 Introduction

Sea-ice is one of the largest biomes on the planet. It has a strong impact on climate through its modulation of heat, water vapour and momentum exchanges, and via the physics (stratification, mixing) and biology (sea-ice and pelagic communities) of the polar regions (Thomas and Dieckman, 2010). In the last decade, seasonal sea-ice loss, associated with atmospheric warming, air–sea-ice feedbacks and climate modes of variability has increased significantly in the Arctic Ocean since 2007 (e.g. ACIA, 2005; Serreze and Francis, 2006; Maslanik et al., 2007; Wang and Overland, 2009). Rapid loss of summertime sea-ice, combined with other synergistic impacts such as hydrological changes (e.g. increased melt and fresh water inputs to polar waters), has profound implications for the biology and physico-biogeochemical conditions of the Arctic and Antarctic seas (e.g. McGuire et al., 2006, 2009; Arrigo et al., 2008; Pabi et al., 2008).

The polar and subpolar regions of both hemispheres have large impacts on the exchange of carbon dioxide (CO<sub>2</sub>) between the atmosphere and ocean, with unclear implications for the uptake and storage of anthropogenic CO<sub>2</sub> in the ocean (e.g. Sabine and Tanhua, 2010; Tanhua et al., 2013). In the high latitudes, ocean CO<sub>2</sub> sinks represent a significant contribution to the global ocean sink of  $\sim 1.4 \text{ Pg C yr}^{-1}$  ( $\text{Pg C} = 10^{15} \text{ g C}$ ; e.g. Takahashi et al., 2009; Schuster et al., 2013). The presence of low temperatures in the Arctic Ocean and seasonally reduced seawater  $p\text{CO}_2$  due to high rates of primary productivity on several shallow continental shelves of the region facilitates substantial ocean uptake of CO<sub>2</sub> from the atmosphere (e.g. Bates and Mathis, 2009). However, quantifying and understanding the present and future dynamics of ocean-atmosphere exchanges of CO<sub>2</sub> in permanently and seasonally ice-covered regions has been difficult to assess owing to a lack of data (e.g. Bates and Mathis, 2009) and uncertainty in the forthcoming trajectory of environmental change such as rapid sea-ice loss and warming, particularly in the Arctic Ocean.

Over the last decade, a limited number of investigations in the Arctic and Antarctica have been conducted on sea-ice CO<sub>2</sub>-carbonate chemistry, the impact of sea-ice on the carbon cycle, and ocean-atmosphere CO<sub>2</sub> exchanges (e.g. Semiletov et al., 2004; Zemmellink et al., 2006; Rysgaard et al., 2007; Delille et al., 2007; Miller et al., 2011a, b; Rysgaard et al., 2011; Fransson et al., 2011; Geilfus et al., 2012a, b; Sogaard et al., 2013). These studies have shown large heterogeneity and variability (in time, space and vertically within sea-ice) in CO<sub>2</sub>-carbonate chemistry in brines and sea-ice of both Arctic and Antarctic environments (Table 1). From these studies, it appears that the dynamics of CO<sub>2</sub> in sea-ice and impacts on ocean-atmosphere exchanges of CO<sub>2</sub> is highly complex and unpredictable. The CO<sub>2</sub>-carbonate chemistry composition of sea-ice is not only a function of physical conditions (i.e. temperature, salinity, ice thickness), and concentration/dilution processes associated with brine formation, brine rejection and ice melt, respectively. It is also a function of sea-ice biological processes such as primary production and respiration (e.g. Gosselin et al., 1986; Legendre et al., 1992; Thomas and Dieckmann, 2010; Dieckmann and Hellmer, 2010), and production of calcium carbonate (CaCO<sub>3</sub>, e.g. ikaite formation; Papadimitriou et al., 2004; Dieckmann et al., 2008; Papadimitriou et al., 2013) and its dissolution. Although few studies on sea-ice and brines have been conducted, there are even fewer studies of CO<sub>2</sub>-carbonate chemistry from above-ice melt ponds or below-ice interface melt waters (i.e. Geilfus et al., 2012a).

Two scenarios, both of which have commonalities and differences, appear relevant to understanding variability in sea-ice CO<sub>2</sub>-carbonate chemistry and impacts on ocean-atmosphere CO<sub>2</sub> exchanges across the seawater-ice-atmosphere interface (Table 1). During freeze-up, the formation of high-salinity brines appears to drive a large uptake of CO<sub>2</sub> from the atmosphere and downward flux of dissolved

inorganic carbon with cold dense waters formed during brine rejection (e.g. Anderson et al., 2004; Omar et al., 2005; Rysgaard et al., 2007). At the same time, very high  $p\text{CO}_2$  (partial pressure of CO<sub>2</sub>;  $> 1000 \mu\text{atm}$ ) values have been reported (Matsuo and Miyake, 1966; Tison et al., 2002; Miller et al., 2011a, b) in both brines and sea-ice. High  $p\text{CO}_2$  conditions in winter sea-ice appear to facilitate efflux of CO<sub>2</sub> from sea-ice into the atmosphere (Miller et al., 2011b). Subsequent melt water produced during spring ice melt may have high  $p\text{CO}_2$  concentrations resulting in loss of CO<sub>2</sub> to the atmosphere from melt ponds and mixed layers that are highly influenced by melt water (e.g. Cooper et al., 2014).

An alternative scenario is that sea-ice and brines have low  $p\text{CO}_2$  contents during sea-ice retreat and melt with strong influx of CO<sub>2</sub> into melt ponds and post-ice-breakup mixed layers (Table 1). Actual direct measurements of  $p\text{CO}_2$  and pH were rarely reported in the original literature but using data from several studies (Rysgaard et al., 2007; Delille et al., 2007; Fransson et al., 2011; Sejr, et al., 2011; Geilfus et al., 2012a),  $p\text{CO}_2$ , pH and saturation states for CaCO<sub>3</sub> minerals can be calculated from reported salinity, temperature and CO<sub>2</sub>-carbonate chemistry data. Such data show strong evidence for very low  $p\text{CO}_2$  ( $< 100 \mu\text{atm}$ ) and high pH ( $> 8.6$ ) in spring sea-ice and brines (Table 1).

In this study, we report CO<sub>2</sub>-carbonate chemistry data from above-ice melt ponds, below-ice interface melt water, and mixed-layer seawater beneath sea-ice cover at 19 sea-ice locations in the western Arctic Ocean. These sea-ice stations were conducted as part of the NASA ICESCAPE (Impacts of Climate on the Eco-Systems and Chemistry of the Arctic Pacific Environment) project, and represent conditions observed in early summer (i.e. July) in 2010 and 2011. Previous studies of CO<sub>2</sub>-carbonate chemistry data from above-ice melt ponds and below-ice interface melt water have been very limited in number to date (e.g. Miller et al., 2011a; Fransson et al., 2011; Geilfus et al., 2012a). It is important to consider the influence of melt ponds on the regional and global ocean carbon cycle given their widespread seasonal distributions. For instance, during the brief sea-ice retreat period, melt ponds can constitute as much as 50% of the surface area (e.g. Sejr et al., 2011). Furthermore, changes in sea-ice distributions associated with warming and other feedbacks in the high latitudes are rapidly changing the complex associations between sea-ice, melt water and seawater in polar regions with profound implications for the global carbon cycle (e.g. Bates and Mathis, 2009). We discuss data collected as part of the ICESCAPE expedition in 2010 and 2011, in the context of other brine and sea-ice studies, to evaluate the possible contribution of sea-ice for CO<sub>2</sub> dynamics and ocean-atmosphere CO<sub>2</sub> exchanges. The potential impact of melt waters on the CO<sub>2</sub>-carbonate chemistry of the underlying mixed layer is also discussed. Finally, we also compare and contrast melt pond and interface water pH and saturation states ( $\Omega$ ) for CaCO<sub>3</sub> minerals – i.e. for aragonite ( $\Omega_{\text{aragonite}}$ ) and calcite ( $\Omega_{\text{calcite}}$ ). The context for this latter discussion

**Table 1.** Summary of measured and calculated  $p\text{CO}_2$  values reported in sea-ice brine, sea-ice and melt ponds. The studies are arranged in seasonal order from fall to spring observations where possible. In most cases,  $p\text{CO}_2$ , pH,  $\Omega_{\text{calcite}}$ , and  $\Omega_{\text{aragonite}}$  were calculated from TA and DIC, or from  $p\text{CO}_2$  and pH. In the cases where values were reported in the original study, salinity and temperature values of 4 and 0 °C were used in the calculations. Where possible, ranges are given or calculation of mean observations reported in the original literature. Please note that the ranges of pH are in reverse order to  $p\text{CO}_2$  to reflect the end-member ranges of high  $p\text{CO}_2$ /low pH and low  $p\text{CO}_2$ /high pH.

Study	Location	Period	Season	$p\text{CO}_2$ ( $\mu\text{atm}$ )	pH	$\Omega_{\text{calcite}}$	$\Omega_{\text{aragonite}}$	Notes
<b>Brine</b>								
Miller et al. (2011a)	Arctic	Nov to Dec	Fall	< 1	12.4	22.5	4.6	2
Miller et al. (2011b)	Arctic	Dec to Mar	Winter	~ 800–12 000	8.2 to 7.1	11.9–1.3	0.8–7.4	1, 6
Miller et al. (2011b)	Arctic	Apr to Jun	Spring	~ 800–12 000	8.2 to 7.1	1.3–11.9	0.8–7.4	1, 6
Geilfus et al. (2012a)	Arctic	Apr	Spring	465–1834	8.0	3.0	1.6	1, 3, 4
Geilfus et al. (2012a)	Arctic	May	Spring	147–888	8.2	1.5	< 0.1	1, 3, 4, 5
Delille et al. (2007)	Antarctic	Nov	Spring	~ 100	9.42	> 20	> 6	1, 3, 5
Delille et al. (2007)	Antarctic	Dec	Spring	~ 420	8.38	3.4	1.8	1, 3, 5, 7
Geilfus et al. (2012a)	Arctic	Jun	Spring	0–180	8.3	0.1	< 0.1	1, 4, 5
Fransson et al. (2011)	Antarctic	Dec to Jan	Spring	9–210	9.3–8.3	3.7–14.8	2.3–9.3	2
<b>Sea-ice</b>								
Miller et al. (2011a)	Arctic	Nov to Dec	Fall	< 1	8.20	0.42	0.25	2, 8, 10
Miller et al. (2011a)	Arctic	Nov to Dec	Fall	< 1	8.97	1.75	0.96	2, 9, 10
Rysgaard et al. (2007)	Arctic	Mar	Spring	< 1–6	9.1–10.4	1.6–5.5	0.86–3.0	2, 10
Miller et al. (2011b)	Arctic	Apr to Jun	Spring	103–197	7.7–7.97	< 0.1	< 0.1	2
Sejr et al. (2011)	Greenland	Mar/Apr	Spring	165 and 195				1, 7
Rysgaard et al. (2007)	Arctic	Apr	Spring	204–522	7.36–7.8	< 0.05	< 0.05	2, 10
Delille et al. (2007)	Antarctic	Nov to Dec	Spring	< 10–420	8.0–8.7	0.5–0.35	0.3–0.19	1, 3, 5
Sogaard et al. (2013)	Arctic	Apr	Spring	< 2 to ~ 10				2, 4
Sogaard et al. (2013)	Arctic	May	Spring	~ 5 to ~ 145				2, 4
Geilfus et al. (2012a)	Arctic	Jun	Spring	50–1800	8.4–6.27	$0.56 \leq 0.1$	$0.3 \leq 0.1$	1
Fransson et al. (2011)	Antarctic	Dec to Jan	Spring	< 10	9.3	14.8	9.3	2
Rysgaard et al. (2011)	Arctic	not given	Spring	< 1	10.0	< 0.1	< 0.1	2
Rysgaard et al. (2011)	Antarctic	not given	Spring	< 1	10.0	< 0.1	< 0.1	2
<b>Melt ponds</b>								
Geilfus et al. (2012a)	Arctic	Jun	Spring	79 to 348	n/a	n/a	n/a	2
This study (acidic type)	Arctic	Jun/Jul	Spring	355–1516	7.4–6.1	< 0.1	< 0.1	2
This study (alkaline)	Arctic	Jun/Jul	Spring	< 1 to 60	10.8–8.6	2.6 to 0.2	1.5 to < 0.1	2

Notes: 1. Direct measurements of  $p\text{CO}_2$ ; 2. calculated here from DIC and TA values reported in the paper using the same dissociation constants as this paper; 3. seasonal decrease in either brines or sea-ice observed; 4. higher  $p\text{CO}_2$  values in deeper part of sea-ice core; 5. also calculated from pH and TA values reported in the paper using the same dissociation constants as this paper; 6. calculated  $p\text{CO}_2$  values from discrete DIC and TA values of up to 45 000  $\mu\text{atm}$  are reported in Miller et al. (2011b); 7. lower  $p\text{CO}_2$  in first-year ice compared to new ice; 8. thin ice (< 15 cm); 9. thick ice (> 15 cm); 10. average values.

is that ocean acidification is expected to impact the polar oceans earlier than other regions (owing to low temperatures and high buffering capacity of surface waters) and given recent observations of low  $\Omega$  waters in surface waters of the Canada Basin (Jutterstrom et al., 2010).

## 2 Methods

### 2.1 Seawater CO<sub>2</sub>–carbonate chemistry considerations

It is useful to briefly summarize the terms and equations governing seawater CO<sub>2</sub>–carbonate chemistry, as this is important context for the discussion of results later in the paper. DIC is the sum of bicarbonate [ $\text{HCO}_3^-$ ], carbonate [ $\text{CO}_3^{2-}$ ] and CO<sub>2</sub> in natural waters (Dickson et al., 2007)

and is thus defined as

$$\text{DIC} = [\text{HCO}_3^-] + [\text{CO}_3^{2-}] + [\text{CO}_2^*], \quad (1)$$

where [ $\text{CO}_2^*$ ] is equivalent to  $[\text{CO}_2]_{\text{aq}} + [\text{H}_2\text{CO}_3]$ . Total alkalinity (TA) can be defined as

$$\begin{aligned} \text{TA} = & [\text{HCO}_3^-] + 2[\text{CO}_3^{2-}] + [\text{B}(\text{OH})_4^-] + [\text{OH}^-] \\ & + [\text{HPO}_4^{2-}] + 2[\text{PO}_4^{3-}] + [\text{SiO}(\text{OH})_3^-] + [\text{NH}_3] + [\text{HS}^-] \\ & + \dots - [\text{H}^+] - [\text{HSO}_4^-] - [\text{HF}] - [\text{H}_3\text{PO}_4], \dots, \end{aligned} \quad (2)$$

where  $[\text{B}(\text{OH})_4^-]$  is total borate concentration in seawater and “...” reflects other minor contributors to alkalinity (Dickson et al., 2007). Equation (2) is a simplified definition of alkalinity with a full description of TA and CO<sub>2</sub>–carbonate chemistry detailed elsewhere (e.g. Stumm and

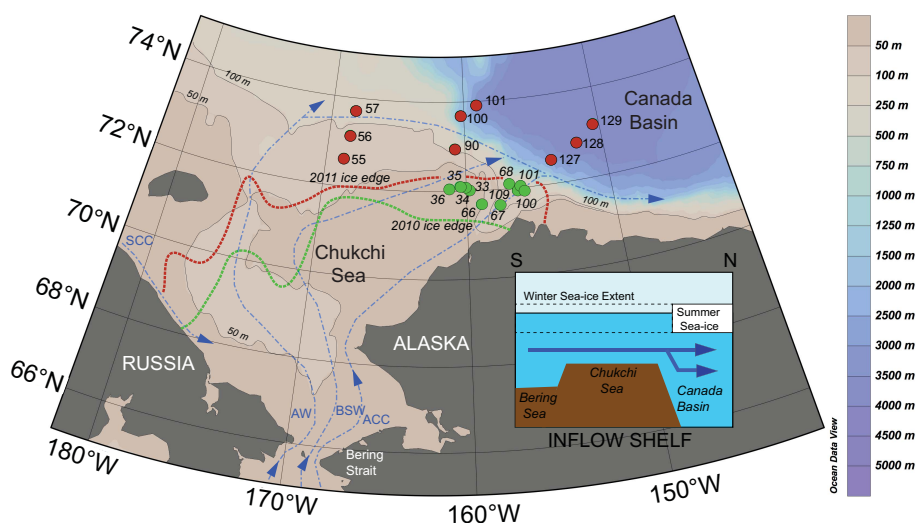


**Figure 1.** Map of the western Arctic Ocean showing the sea-ice stations occupied during the ICESCAPE cruises of 2010 (red symbols) and 2011 (green symbols) with sea-ice station numbers also shown. The approximate sea-ice edge is shown for 2010 (bold dashed green line) and 2011 (bold dashed red line). Approximate streamlines (blue dashed lines) of water flow across the Chukchi Sea are shown and include the following water masses: Alaskan Coastal Current (ACC), Bering Shelf Water (BSW) and Anadyr Water (AW). The intermittent flow of the Siberian Coastal Current (SCC) through Long Strait into the Chukchi Sea is also shown. Sea ice data were retrieved from the National Sea-Ice Data Center (Cavalieri et al., 1996, updated yearly; <http://nsidc.org/data/seaice/index>). INSET. A schematic of the “inflow” shelf is shown illustrating the northward flow of water across the shelf from the Bering Sea, through Bering Strait, and across the Chukchi Sea shelf to the Canada Basin.

Morgan, 1981; Butler, 1992; Zeebe and Wolf-Gladrow, 2011; Dickson et al., 2007). All components of the seawater CO<sub>2</sub>–carbonate system, including [HCO<sub>3</sub><sup>-</sup>], [CO<sub>3</sub><sup>2-</sup>] and saturation states for CaCO<sub>3</sub> minerals such as calcite ( $\Omega_{\text{calcite}}$ ) and aragonite ( $\Omega_{\text{aragonite}}$ ), can be computed from two observed parameters. DIC, TA, pH and  $p\text{CO}_2$  are the common measurable parameters.

Physico-biogeochemical processes such as ocean release of CO<sub>2</sub> by air–sea gas exchange or primary production act to decrease DIC and  $p\text{CO}_2$  and increase pH,  $\Omega_{\text{aragonite}}$  and  $\Omega_{\text{calcite}}$  (e.g. Zeebe and Wolf-Gladrow, 2001). In contrast, ocean uptake of CO<sub>2</sub> and respiration act oppositely (increasing DIC and  $p\text{CO}_2$  and decreasing pH,  $\Omega_{\text{aragonite}}$  and  $\Omega_{\text{calcite}}$ ), while TA remains unchanged (except for minor changes associated with nitrate uptake or release; Brewer and Goldman, 1976; Dickson et al., 2007). Precipitation or calcification and dissolution of CaCO<sub>3</sub> is defined as



Calcification / CaCO<sub>3</sub> precipitation decreases TA, while CaCO<sub>3</sub> dissolution increases TA, respectively.

## 2.2 Sampling and chemical analyses

### 2.2.1 Water column sampling

The hydrography and biogeochemistry of the western Arctic Ocean was sampled during two ICESCAPE cruises aboard the US Coast Guard (USCGC) conducted in early summer of 2010 and 2011. In 2010, 140 hydrocast-CTD stations were occupied (18 June to 16 July 2011), while 173 hydrocast-CTD stations were occupied in 2011 (28 June to 24 July 2011). Water column sampling was mainly conducted on the shallow shelf of the Chukchi Sea but also in the deep (> 200 m depth) southern Canada Basin. Core hydrography samples (e.g. salinity, temperature, inorganic nutrients, chlorophyll *a*) were collected as well as ~1600 water column seawater samples for DIC and TA. Inorganic nutrients and chlorophyll *a* (along with other pigments) were measured with autoanalyser and HPLC techniques, respectively (e.g. Arrigo et al., 2012, 2014).

The majority of the sampling occurred on the shallow shelf of the Chukchi Sea (~30 to ~70 m deep, plus shelf-break samples as deep as 200 m) during the summertime sea-ice retreat period (Fig. 1). The shelf has been characterized as an inflow shelf (Carmack and Wassmann, 2006; Fig. 1 inset) in which the physical and hydrographic properties are highly influenced by the northward flow of nutrient rich North Pacific Ocean water associated with transports of Anadyr Water (AW), Bering Shelf (BSW) and Alaskan Coastal Current (ACC) waters from the Bering Sea to the Canada Basin.

### 2.2.2 Sea-ice Stations

Nineteen sea-ice stations were occupied during the ICESCAPE expedition, ten in 2010 (covering the period of 24 June to 11 July) and nine in 2011 (covering the period of 5 to 20 July; Fig. 1). Most of the sea-ice stations were located over the Chukchi Sea shelf but several were also located in the deep Canada Basin. At each of the sea-ice stations, samples were collected from above-ice melt ponds, below-ice ice–water interface and in the surface mixed layer beneath. Sampling on the ice was conducted upwind of the ship at representative ice stations (Frey et al., 2012; unpublished data). Sea-ice melt pond water was sampled for salinity, temperature, inorganic nutrients and seawater CO<sub>2</sub>–carbonate chemistry. Nearby, ice cores were drilled and under-ice seawater (at the ice–water interface within 0.1 m of the ice bottom) was sampled for water chemistry using a vertically oriented Kemmerer water sampler. At each ice station, CTD-hydrocast (using Niskin samplers) sampling of the water column was undertaken from the USCGC *Healy* after ice operations were completed. In situ temperature was measured at each station.

Melt pond water, interface melt water, and CTD-hydrocast salinity samples were analysed onboard the USCGC *Healy* after sampling with a Guildline salinometer (calibrated with seawater salinity standards) as part of the core hydrography measurement suite. Chlorophyll *a* values of melt pond waters were measured using HPLC techniques.

DIC and TA samples, collected in ~ 300 mL Pyrex bottles that were poisoned with 100 µL Hg<sub>2</sub>Cl<sub>2</sub>, sealed and stored in the dark before analysis, were analysed onboard the vessel. The exception was that DIC samples from 2010 were analysed at UAF. Replicate samples were also analysed at BIOS within a few months of sampling.

### 2.2.3 Chemical analyses

DIC was determined using a high-precision (0.05 %CV) small-volume DIC analyser (~ 1.5 mL sample size) using an infrared-based instrument (AIRICA; Marianda Co., Germany). TA was determined by a high-precision (< 0.05 %CV) potentiometric technique using a VINDTA 2S (Marianda Co., Germany). Multiple replicates samples were analysed and analytical imprecision was less than 0.1 % (~ 2 µmol kg<sup>-1</sup>). Both DIC and TA analyses were routinely calibrated using seawater Certified Reference Material (CRM) from A.G. Dickson, Scripps Institute of Oceanography, and the accuracy of samples compared to CRM's was less than 0.1 % (~ 2 µmol kg<sup>-1</sup>). Six samples of sea-ice (three from multi-year and three from first-year ice) were also collected in gas tight bags, carefully melted and analysed for DIC onboard the USCGC *Healy* in 2011. Given the lack of low-salinity (< 30), low TA (< 2000 µmol kg<sup>-1</sup>) CRMs, an assumption is made that the calibration fit for TA from higher TA values from CRMs remains robust for low

salinity waters encountered in the Arctic Ocean. This assumes that TA remains conservative relative to salinity and ionic strength, and that minor changes in activity coefficients across the range of ionic strength (e.g. Butler et al., 1982) does not significantly alter the ion balance of the alkalinity term.

### 2.3 Data computations and visualization

Seawater CO<sub>2</sub>–carbonate system parameters including *p*CO<sub>2</sub> (µatm), Ω<sub>aragonite</sub> and Ω<sub>calcite</sub> and pH (total scale) were computed from salinity (*S*), temperature (*T*, °C), TA and DIC data (using CO2calc software; Robbins et al., 2011). The carbonic acid dissociation constants *p*K<sub>1</sub> and *p*K<sub>2</sub> (Mehrbach et al., 1973 as refit by Dickson and Millero, 1987) were used to allow better calculations at the low temperatures present in the Arctic Ocean. We estimated the calculation error range for *p*CO<sub>2</sub>, pH, Ω<sub>aragonite</sub> and Ω<sub>calcite</sub> to be +5 µatm, +0.001 and +0.004 (assuming analytical imprecision for DIC at ±0.5 µmol kg<sup>-1</sup> and for TA at 2 µmol kg<sup>-1</sup>), respectively. For low-salinity waters, a threefold larger inaccuracy is estimated for TA analyses and computation of other components of the CO<sub>2</sub>–carbonate system, and an error of 5 % is allowed for in the computation of *p*CO<sub>2</sub>, pH, Ω<sub>aragonite</sub> and Ω<sub>calcite</sub> in melt pond waters. In a previous study, Delille et al. (2007) demonstrated no difference between measured and calculated *p*CO<sub>2</sub> (from DIC and TA measurements) in low-salinity sea-ice samples using the same dissociation constants as used in this study. The relatively good 1 : 1 fit of measured and calculated *p*CO<sub>2</sub> as shown from the Delille et al. (2007) study also suggests that TA in low-salinity waters such as sea-ice and melt ponds appear not to be influenced by non-conservative behaviour of cations and anions that contribute to alkalinity.

Ocean Data View 4 (ODV; Schlitzer, 2011) software was used to visualize the data. We also used reported salinity, temperature and seawater CO<sub>2</sub>–carbonate chemistry (typically DIC and TA) from the few studies of brines and sea-ice (e.g. Rysgaard et al., 2007, 2011; Fransson et al., 2011; Miller et al., 2011a, b; Geilfus et al., 2012a; Sogaard et al., 2013) to compute *p*CO<sub>2</sub>, pH, Ω<sub>aragonite</sub> and Ω<sub>calcite</sub> (Table 1) that were not reported in the original literature. The solubility of ikaite in sea-ice has also been determined recently (Papadimitriou et al., 2013) but not yet incorporated into the CO2calc software of Robbins et al. (2010). Since ikaite is slightly more soluble than aragonite, Ω<sub>aragonite</sub> is used in the text.

## 3 Results

### 3.1 Shelf hydrography and biogeochemical properties

At the time of the two cruises (late June to mid July), most of the Chukchi Sea was sea-ice free with sea-ice cover restricted to the northernmost regions of the shelf and slope,

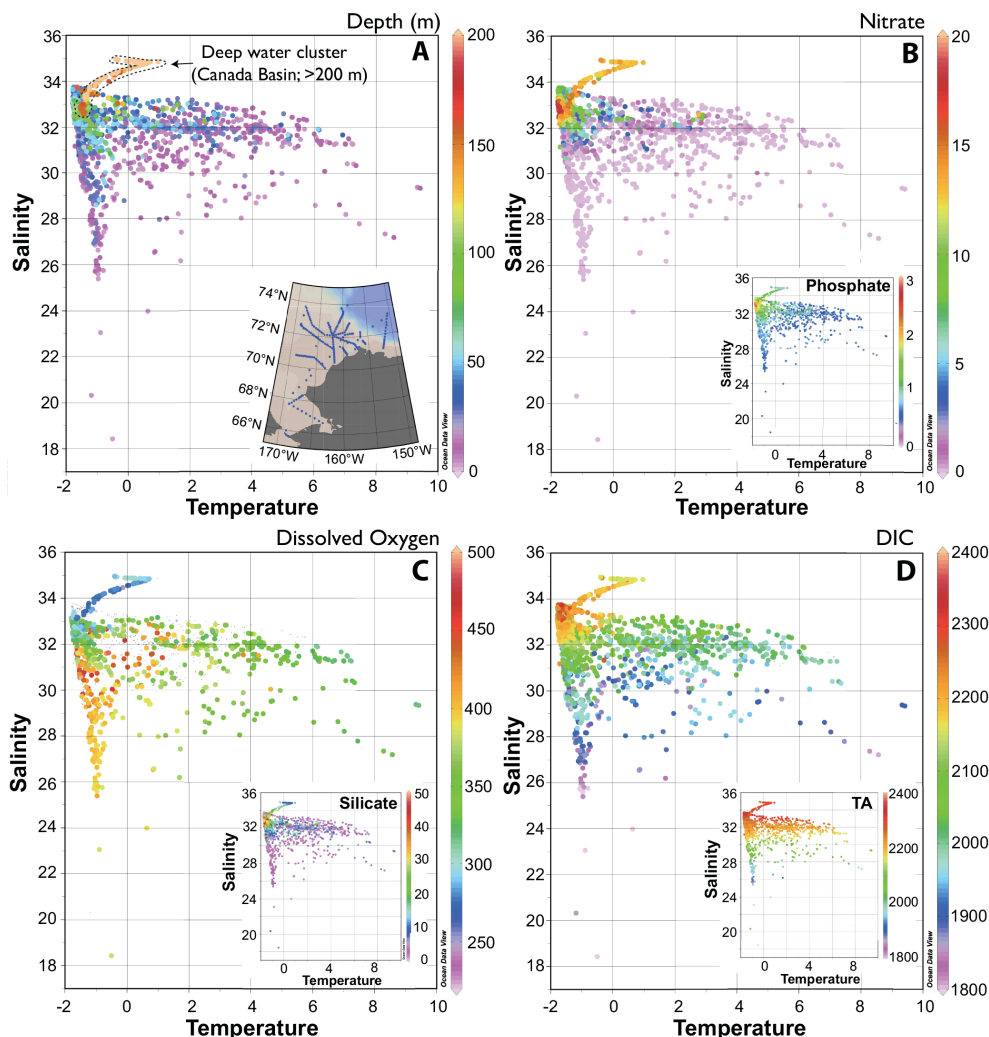


**Figure 2.** Water column hydrography and marine biogeochemistry of the 2010 and 2011 ICESCAPE cruises. **(a)** Temperature (°C) versus salinity with range of colour denoting depth (in metres), and locations of 2010 and 2011 ICESCAPE hydrocast-CTD stations shown in the inset. The depth of samples collected below 200 m is not differentiated colourwise, and represents water depths to > 4000 m. With this in mind, the approximate range of deep water (Canada Basin) hydrographic properties are shown within the dashed line. **(b)** Temperature (°C) versus salinity with range of colour denoting nitrate concentration ( $\mu\text{mol kg}^{-1}$ ) with phosphate ( $\mu\text{mol kg}^{-1}$ ) shown in the inset. **(c)** Temperature (°C) versus salinity with range of colour denoting dissolved oxygen concentration ( $\mu\text{mol kg}^{-1}$ ) with silicate ( $\mu\text{mol kg}^{-1}$ ) shown in the inset. **(d)** Temperature (°C) versus salinity with range of colour denoting dissolved inorganic carbon (DIC) concentration ( $\mu\text{mol kg}^{-1}$ ) with total alkalinity (TA;  $\mu\text{mol kg}^{-1}$ ) shown in the inset.

and the southern Canada Basin (Fig. 1). Most of the Chukchi Sea shelf is shallower than 100 m (Fig. 2a), while the Canada Basin was sampled to depths > 4000 m (Fig. 2 inset). A wide range of temperature ( $-1.8$  to  $\sim 8$  °C) and salinity ( $\sim 27$  to 33; Fig. 2a) was observed over the shelf in both summers of 2010 and 2011. As reported elsewhere (Bates et al., 2013), winter/early spring water (including remnant winter water on the shelf during summertime; Spall et al., 2014) had a narrow range of temperature ( $-1.8$  to  $< -1$  °C) and salinity ( $\sim 32.2$  to 32.8), with summertime variability in shelf water mixed-layer temperature and salinity reflecting the influence of warming and sea-ice melt. The hydrographic properties of

shelf water exhibited two generic water mass types, including: (1) high salinity (32 to 33) and variable temperature ( $-1$  to 8 °C), and (2) variable salinity (26 to 33) and cold temperature ( $-1.8$  to  $< 1$  °C), with variability in between these two water mass types. The freshest mixed-layer salinity was about 18 (Fig. 2a).

Shelf waters generally had relatively low nitrate ( $< 6 \mu\text{mol kg}^{-1}$ ) and phosphate ( $< 1 \mu\text{mol kg}^{-1}$ ) concentrations, compared to nutrient-rich winter/early-spring shelf water and deep Canada Basin waters (Fig. 2b). Similar patterns were shown in silicate for shelf waters ( $< 5$  to  $10 \mu\text{mol kg}^{-1}$ ) with high dissolved oxygen concentrations

(350–450  $\mu\text{mol kg}^{-1}$ ). This likely reflects the production of dissolved oxygen on the Chukchi Sea shelf from high rates of pelagic primary production and during summertime (e.g. Hameedi, 1978; Cota et al., 1996; Wheeler et al., 1996; Chen et al., 2002; Hill and Cota, 2005; Bates et al., 2005a; Mathis et al., 2008a) and potentially some contribution from growth of the biological community in sea-ice. In contrast to nitrate and phosphate distributions, both silicate and dissolved oxygen in the deep Canada Basin water had lower concentrations than the remnant winter/early-spring water (beneath the mixed layer of  $\sim 15$  to 25 m depth) on the shelf and slope waters of the Chukchi Sea.

### 3.2 Water column seawater CO<sub>2</sub>–carbonate chemistry on the Chukchi Sea shelf

Winter/early-spring water (including winter water remnant on the shelf during summertime) and deep Canada Basin water had a narrow range of DIC ( $\sim 2200$  to  $2300 \mu\text{mol kg}^{-1}$ ) and TA ( $\sim 2250$  to  $2350 \mu\text{mol kg}^{-1}$ ). In contrast, summertime shelf waters had a large range of seawater CO<sub>2</sub>–carbonate chemistry with DIC ranging from  $\sim 1850$  to  $2300 \mu\text{mol kg}^{-1}$  and TA ranging from  $1850$  to  $2350 \mu\text{mol kg}^{-1}$ , respectively (Fig. 2d).

A closer inspection of the data revealed that surface/mixed-layer DIC and TA had a smaller range of  $\sim 1800$  to  $2000$  and  $1850$  to  $2250 \mu\text{mol kg}^{-1}$ , respectively (Fig. 3a), over a salinity range of 6 (Fig. 3a inset). These shelf waters generally had high dissolved oxygen contents ( $\sim 350$  to  $> 450 \mu\text{mol kg}^{-1}$ ) and low nitrate values ( $< 3 \mu\text{mol kg}^{-1}$ , Fig. 3b), reflecting uptake of nitrate in support of primary and new production and generation of oxygen as a result (e.g. Hill and Cota, 2005; Bates et al., 2005a; Arrigo et al., 2012).

Shelf-surface/mixed-layer seawater  $p\text{CO}_2$  generally had low values ( $< 100$  to  $300 \mu\text{atm}$ ; Fig. 3c) relative to atmospheric  $p\text{CO}_2$  values of  $\sim 392$  to  $398 \mu\text{atm}$ . As shown in previous studies (e.g. Pipko et al., 2002; Murata et al., 2003; Bates, 2006; Bates et al., 2006; Bates and Mathis, 2009), several factors including summertime undersaturation of CO<sub>2</sub> relative to the atmosphere, retreat of sea-ice cover, and moderate to strong winds act in combination as strong driving forces for ocean sinks of CO<sub>2</sub> from the atmosphere. In contrast to shelf-surface/mixed-layer, deeper remnant winter water on the shelf and deep waters of the Canada Basin had higher and much larger ranges of seawater  $p\text{CO}_2$  ( $\sim 300$  to  $> 600 \mu\text{atm}$ ; Fig. 3c). Deeper water (particularly in halocline waters of the Canada Basin) had the highest  $p\text{CO}_2$  values (up to  $1300 \mu\text{atm}$ ).

Shelf-surface/mixed-layer seawater pH had a relatively large range ( $\sim 8.2$  to  $8.5$ ) in contrast to lower pH in deeper waters ( $< 7.8$ ; Fig. 3c inset). Relatively high pH of surface water on the Chukchi Sea shelf, when compared to typical open-ocean pH values of  $8.1$  to  $8.2$ , reflected the impact of high rates of primary production on the shelf on CO<sub>2</sub>–

carbonate chemistry. As shown for the Chukchi Sea (e.g. Bates et al., 2009, 2013), as well as other marine environments, photosynthetic uptake of CO<sub>2</sub> increases pH due to adjustment of seawater CO<sub>2</sub> equilibrium (e.g. Zeebe and Wolf-Gladrow, 2002; Dickson et al., 2007). The saturation state values for CaCO<sub>3</sub> minerals such as aragonite (i.e.  $\Omega_{\text{aragonite}}$ ) and calcite (i.e.  $\Omega_{\text{calcite}}$ ) ranged from  $\sim 0.5$  to  $4.0$  with a few values less than 1 (Fig. 3d). As shown in Fig. 3d,  $\Omega$  values less than 1 for aragonite for some shelf waters and deep waters in the Canada Basin indicated that these waters were potentially corrosive for CaCO<sub>3</sub>.

### 3.3 Above-ice melt and interface seawater CO<sub>2</sub>–carbonate chemistry

Nineteen sea-ice stations were sampled for seawater CO<sub>2</sub>–carbonate chemistry in 2010 and 2011. Both above-ice melt ponds and below-ice interface melt waters were sampled and compared to mixed-layer conditions beneath each ice station (Figs. 4–6) and water column hydrocast stations.

#### 3.3.1 Salinity and temperature variability

The salinity range of the sampled above-ice ponds ranged from  $0.5$  to  $6$  with one sample in the Canada Basin at  $\sim 16$  (Fig. 4a). The Chukchi Sea shelf melt pond water had lower salinity compared to melt ponds sampled in the Canada Basin (Table 2). The interface water sampled just below the sea-ice had highly variable salinity values (Fig. 4c) compared to above-ice melt pond water (i.e. salinity  $< 5$ ), or the mixed-layer beneath (e.g. salinity  $> 25$ ; Fig. 4e). Interface waters with values in between these end-members reflect varying proportions of mixed-layer and sea-ice melt water contributions (Fig. 4c). The below-ice interface melt waters also had temperature ranges of  $-1.6$  to  $+1.6^\circ\text{C}$ , with a mean of  $-0.97^\circ\text{C}$  across the two regions.

#### 3.3.2 TA and DIC variability

The majority of TA and DIC values for above-ice melt pond water ranged from  $< 50$  to  $600 \mu\text{mol kg}^{-1}$  (Figs. 4b, 5a) and typically lower than interface water or mixed-layer seawater values. The exception to this was the higher salinity melt pond water that had TA and DIC values at  $\sim 1030$  and  $1170 \mu\text{mol kg}^{-1}$ , respectively. As with salinity variations in melt pond water, there were also geographic differences with the Chukchi Sea shelf exhibiting lower TA and DIC compared to the Canada Basin (Table 2; Fig. 4b). The mean DIC of Chukchi Sea shelf melt pond water ( $169 \mu\text{mol kg}^{-1}$ ; Table 2) was similar to the mean DIC content ( $148.2 \pm 54.1 \mu\text{mol kg}^{-1}$ ; range of  $75$  to  $224 \mu\text{mol kg}^{-1}$ ; TA was not measured) of six melted sea-ice cores during ICESCAPE cruises in 2011.

As expected from higher salinity values, the interface water had highly variable TA and DIC contents (Fig. 4d), either having similarities to above-ice melt pond water or the mixed

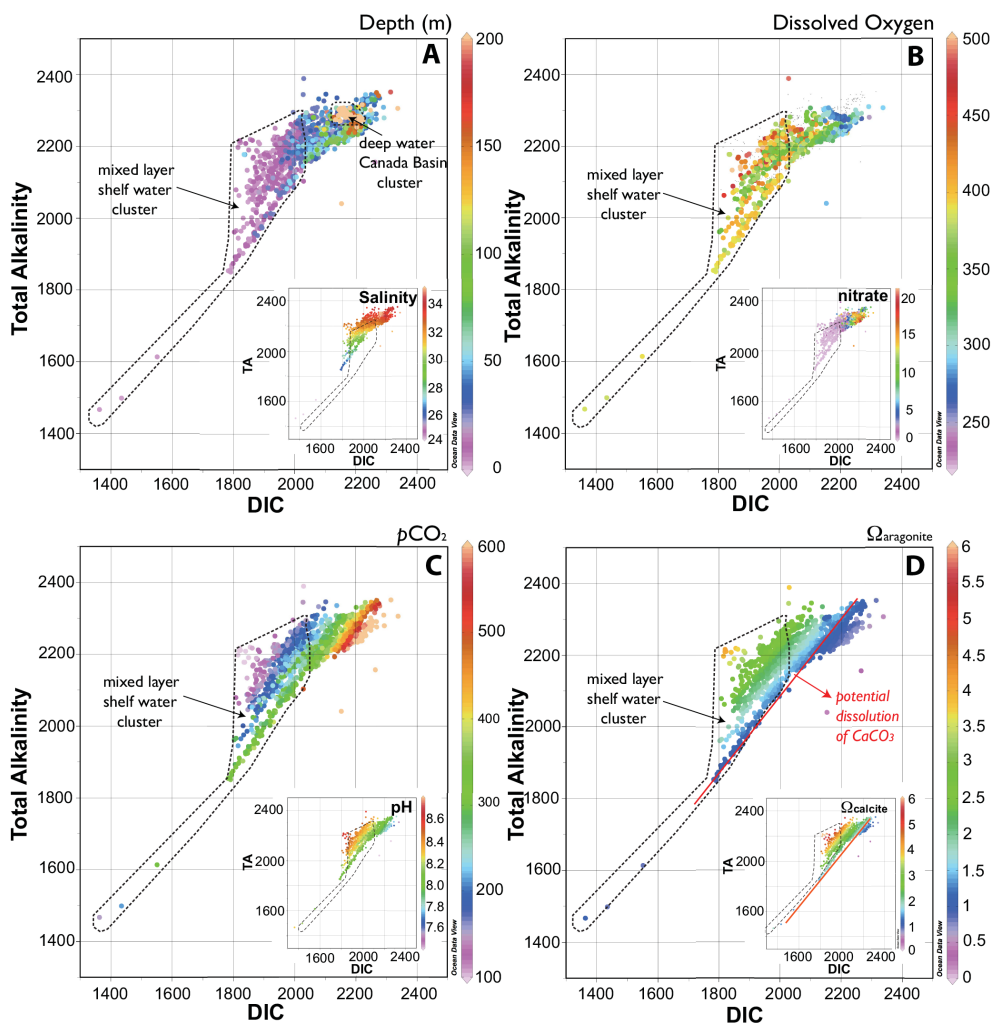


**Figure 3.** Seawater CO<sub>2</sub>–carbonate chemistry and marine biogeochemistry of the 2010 and 2011 ICESCAPE cruises. (a) DIC ( $\mu\text{mol kg}^{-1}$ ) versus total alkalinity (TA;  $\mu\text{mol kg}^{-1}$ ) with range of colour denoting depth (in metres), with salinity shown in the inset. The depth of samples collected below 200 m is not differentiated colourwise, and represents water depth to > 4000 m. With this in mind, the approximate range of deep water (Canada Basin) hydrographic properties are shown within the light dashed line. Approximate cluster of shelf mixed-layer water is shown here and in all panels and insets. (b) DIC ( $\mu\text{mol kg}^{-1}$ ) versus total alkalinity (TA;  $\mu\text{mol kg}^{-1}$ ) with range of colour denoting dissolved oxygen ( $\mu\text{mol kg}^{-1}$ ) with nitrate ( $\mu\text{mol kg}^{-1}$ ) shown in the inset. (c) DIC ( $\mu\text{mol kg}^{-1}$ ) versus total alkalinity (TA;  $\mu\text{mol kg}^{-1}$ ) with range of colour denoting  $p\text{CO}_2$  ( $\mu\text{atm}$ ) with pH (no units) shown in the inset. (d) DIC ( $\mu\text{mol kg}^{-1}$ ) versus total alkalinity (TA;  $\mu\text{mol kg}^{-1}$ ) with range of colour denoting saturation state ( $\Omega$ ) for aragonite (no units) with  $\Omega_{\text{calcite}}$  (no units) shown in the inset. The red line denotes  $\Omega$  values of 1 with potential dissolution of CaCO<sub>3</sub> minerals below a  $\Omega$  value of 1.

layer beneath each ice station (Figs. 4f, 5a). The DIC content of six sea-ice samples was similar to the sea-ice melt pond data ( $\sim 25$  to  $250 \mu\text{mol kg}^{-1}$ ).

### 3.3.3 Above-ice melt pond $p\text{CO}_2$ and pH variability

The above-ice melt pond water had highly variable CO<sub>2</sub>–carbonate chemistry with  $p\text{CO}_2$  values that ranged from < 1 to  $1,500 \mu\text{atm}$  and pH ranges from 6.1 to 8.8 (Figs. 5a, b, 6; Tables 1, 2). Two types of melt pond water were sampled: (1) acidic/neutral type with low pH (6.1 to 7.8) and high

$p\text{CO}_2$  of 355 to  $1516 \mu\text{atm}$ , and; (2) alkaline type with high pH ( $\sim 8.6$  to  $10.8$ ) and low  $p\text{CO}_2$ .

*Chukchi Sea shelf:* The majority of above-ice melt pond water sampled on the Chukchi Sea shelf were of the acidic/neutral type with lower pH values ( $< 7.8$ ; Fig. 6a) and higher  $p\text{CO}_2$  (Fig. 6b) compared to contemporaneous mixed-layer pH and  $p\text{CO}_2$  at the ice stations (Fig. 6e, f). Several melt pond water samples had pH less than 7 (i.e. mildly acidic; Fig. 6a). The mean pH of Chukchi Sea melt pond water was  $7.38 \pm 1.05$  compared to the mean mixed layer at  $8.24 \pm 0.13$  (Table 2). In these acidic/neutral melt pond waters,  $p\text{CO}_2$  values (Fig. 6b) were highly variable

**Table 2.** Summary of mean above-ice and interface water hydrography and CO<sub>2</sub>–carbonate chemistry sampled at the sea-ice stations during the ICESCAPE expeditions in 2010 and 2011 with comparisons to the average mixed layer and remnant winter water conditions beneath the interface waters.

Location Water type	<i>n</i>	Salinity	Temperature	TA (μmoles kg <sup>-1</sup> )	DIC (μmoles kg <sup>-1</sup> )	TA : DIC/ <i>n</i> TA : <i>n</i> DIC	pH	<i>p</i> CO <sub>2</sub> (μatm)	Ω <sub>aragonite</sub>
Chukchi Sea shelf									
Melt pond	14	1.85 ± 1.70	n/a	142.0 ± 117	169.5 ± 130	0.870 : 1.000	7.38 ± 1.05	382 ± 243	0.03 ± 0.06
Interface	14	19.22 ± 9.3	-0.97 ± 0.56	1651.3 ± 69	1542.7 ± 61	1.097 : 1.000	8.53 ± 0.52	148 ± 76	1.78 ± 0.71
Mixed layer	14	30.08 ± 1.05	-0.79 ± 0.95	2115.1 ± 59	1938.4 ± 53	1.091 : 1.000	8.28 ± 0.11	204 ± 68	1.90 ± 0.44
Mixed layer	273	30.72 ± 1.66	1.41 ± 2.36	2151.7 ± 69	1946.8 ± 75	1.105 : 1.000	8.24 ± 0.13	208 ± 131	2.19 ± 0.69
Winter water*	114	32.92 ± 1.66	-1.78 ± 0.15	2269.5 ± 17	2207.0 ± 23	1.028 : 1.000	7.92 ± 0.13	517 ± 142	1.03 ± 0.38
Winter water range	(31.48–33.75)	(-1.78 to -0.98)	(2210–2344)	(2091–2292)	n/a	(7.70–8.41)	(139–851)	(0.62–2.67)	
Canada Basin									
Melt pond	5	5.9 ± 6.4	n/a	476 ± 482	447 ± 442	1.346 : 1.000	8.43 ± 1.68	589 ± 778	0.03 ± 0.06
Interface	5	23.9 ± 2.0	-0.96 ± 0.08	1826.9 ± 77	1728.3 ± 101	1.058 : 1.000	8.18 ± 0.14	247 ± 79	1.15 ± 0.22
Mixed layer	5	26.4 ± 0.7	-0.68 ± 0.63	1916.1 ± 57	1837.9 ± 53	1.043 : 1.000	8.07 ± 0.01	322 ± 13	0.99 ± 0.07

Stations 100, 101, 127, 128, and 129 (see Fig. 1) were deemed Canada Basin sea-ice locations. \* Winter water data refers to bottle data collected between 70 and 73° N on the Chukchi Sea shelf from 30 to 50 m deep during the ICESCAPE 2010 and 2011 cruises. The winter water remnant on the Chukchi Sea has hydrographic properties in the range of winter water defined by Spall et al. (2014). The mean phosphate, silicate, nitrate and dissolved oxygen concentrations (μmol kg<sup>-1</sup>) were 1.77 ± 0.24, 31.2 ± 13.2, 11.83 ± 3.20, and; 311.3 ± 20.4, respectively. A few warmer samples (≥ 0.5 °C) with low nitrate values (< 6 μmoles kg<sup>-1</sup>) were not included as representative of winter remnant water.

(355 to 1,516 μatm) with the mean *p*CO<sub>2</sub> much higher (382 ± 243 μatm; Table 2) than the Chukchi Sea shelf mixed layer (208 ± 131 μatm; Table 2) and closer to contemporaneously measured atmospheric *p*CO<sub>2</sub> values of 392 to 398 μatm.

*Canada Basin:* As shown in Fig. 6b, two acidic/neutral type (with very high *p*CO<sub>2</sub> values of > 1,000 μatm) and several alkaline type melt pond waters were sampled at ice stations in the Canada Basin. All of these alkaline melt pond waters had very low *p*CO<sub>2</sub> values (< 60 μatm; Fig. 5c; Table 1) and pH values higher than 8.6. Higher pH and *p*CO<sub>2</sub> mean values than the mixed layer are reported in Table 2 but with the caveat that the small sample size cannot give a representative view of the proportion of acidic/neutral type or alkaline type melt ponds across the Canada Basin.

### 3.3.4 Interface water pH and *p*CO<sub>2</sub> variability

In comparison to above-ice melt ponds, the below-ice interface water had pH values (> 8; Fig. 6c), closer to values for typical seawater and the underlying mixed-layer water present beneath the ice (Fig. 6e). As with hydrographic and DIC/TA properties, geographic differences in pH and *p*CO<sub>2</sub> between the two areas was evident.

*Chukchi Sea shelf:* In contrast to above-ice melt pond water, Chukchi Sea shelf interface water tended to have higher pH and lower *p*CO<sub>2</sub> (means of 8.53 ± 0.52 and 148 ± 131 μatm, respectively) compared to the underlying mixed layer and mixed layer across the northern Chukchi Sea (Table 2; Fig. 7a). The interface waters of the Chukchi Sea were more alkaline relative to the mixed layer and especially compared to the co-located above-ice melt ponds.

*Canada Basin:* Similar to the Chukchi Sea shelf, the few sampled Canada Basin interface waters had higher pH and lower *p*CO<sub>2</sub> than the underlying mixed layer (Table 2; Fig. 7a). However, compared to the Chukchi Sea shelf in-

terface waters, interface waters of the Canada Basin were less alkaline (a mean pH of 8.18 compared to 8.53; Table 2; Fig. 7a).

### 3.3.5 Above-ice melt and interface water CaCO<sub>3</sub> saturation states

The saturation states for CaCO<sub>3</sub> minerals such as aragonite and calcite in above-ice melt pond and interface waters were highly variable compared to mixed-layer values across the Chukchi Sea shelf.

*Above-ice melt pond water.* Nearly all the melt ponds had Ω<sub>aragonite</sub> values that were less than 0.2 (Fig. 5d; Table 2) at the Chukchi Sea shelf and Canada Basin ice station. Although not shown, the Ω values for calcite (i.e. Ω<sub>calcite</sub>) were also less than 0.2. Such Ω values less than a value of 1 indicate chemical conditions favouring dissolution of CaCO<sub>3</sub>. The ICESCAPE data indicate that nearly all the sampled melt ponds were highly corrosive for any CaCO<sub>3</sub> particles present in melt water. In Table 1, Ω<sub>calcite</sub> and Ω<sub>aragonite</sub> were also calculated for brines and sea-ice chemistry reported in the literature. In these other settings, saturation states for CaCO<sub>3</sub> minerals were also highly variable, exhibiting highly undersaturated low Ω values in acidic type brines and sea-ice, and high Ω values (2 to 22) in alkaline brines and sea-ice.

*Interface water.* The CaCO<sub>3</sub> mineral saturation states of interface waters were highly variable. Most samples had Ω values similar to the underlying mixed layer (Table 2). For the Chukchi Sea shelf, interface waters were oversaturated with respect to CaCO<sub>3</sub> minerals such as aragonite (Ω<sub>aragonite</sub> mean of 1.78 ± 0.71 compared to mixed layer of 2.19 ± 0.69; Table 2) and likely the more metastable ikaite commonly found in sea-ice. The Canada Basin Ω<sub>aragonite</sub> of interface waters were similar to underlying mixed-layer values (Table 2). Previous studies of the mixed layer (e.g. Jutterstrom et al., 2010; Bates et al., 2013) have shown the presence of

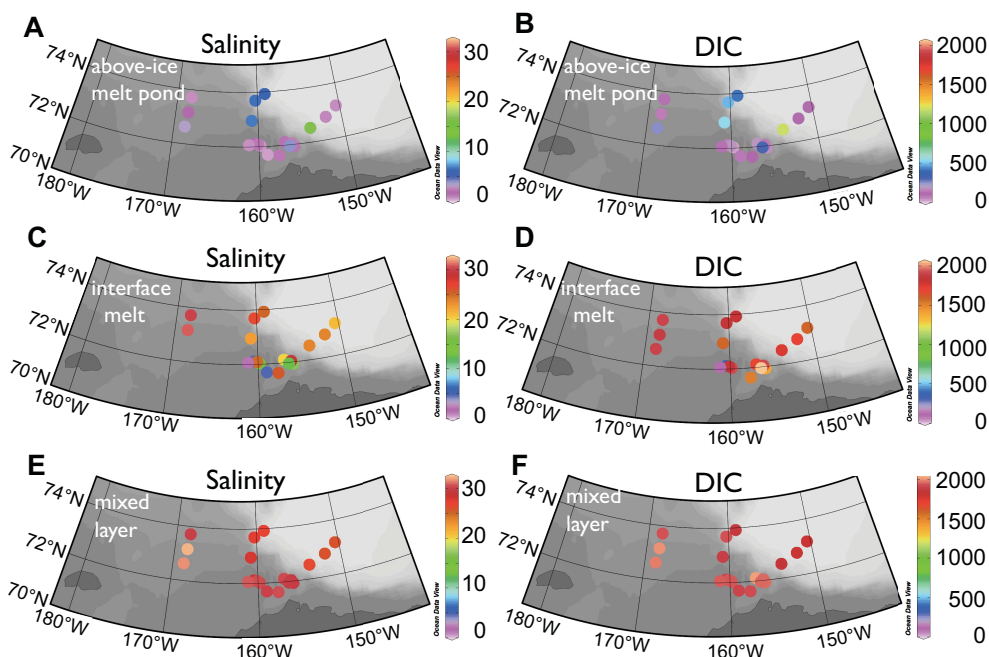


**Figure 4.** Surface maps of above-ice melt ponds, below-ice interface melt water, and mixed-layer values beneath each ice station sampled on 2010 and 2011 ICESCAPE cruises. (a) Salinity for above-ice melt ponds. (b) DIC ( $\mu\text{mol kg}^{-1}$ ) for above-ice melt ponds. (c) Salinity for below-ice interface melt water. (d) DIC ( $\mu\text{mol kg}^{-1}$ ) for below-ice interface melt water. (e) Salinity for mixed-layer values beneath each ice station. (f) DIC ( $\mu\text{mol kg}^{-1}$ ) for mixed-layer values beneath each ice station. Similar panels are shown for TA in Fig. 5.

undersaturated waters with respect to CaCO<sub>3</sub> in the Canada Basin.

## 4 Discussion

### 4.1 Sea-ice melt pond CO<sub>2</sub>–carbonate chemistry

#### 4.1.1 Comparison to other sea-ice settings

The ICESCAPE expeditions in 2010 and 2011 revealed that the CO<sub>2</sub>–carbonate chemistry of melt pond and interface waters was highly variable, and distinctly different from the underlying water column across the Chukchi Sea and Canada Basin.

As discussed in Sect. 3.3, the above-ice melt pond water had two different chemical types: alkaline and acidic/neutral. The alkaline type had much lower  $p\text{CO}_2$  and  $\Omega_{\text{aragonite}}$  values ( $< 50 \mu\text{atm}$  and 0.3–1.5, respectively) and higher pH (8.5 to 10.8; Table 1; Fig. 7b) compared to seawater, presumably reflecting the contribution of alkalinity to melt pond water. In contrast, the acidic/neutral type of above-ice melt pond water had much higher  $p\text{CO}_2$  ( $> 390$  to  $\sim 1500 \mu\text{atm}$ ; Table 1; Fig. 7b) and lower  $\Omega_{\text{aragonite}}$  and pH values ( $< 0.3$  and 6.1 to 7.5, respectively).

How do these melt waters with two different types of CO<sub>2</sub>–carbonate chemistry compare to the water column and other sea-ice environments? In shelf waters of the western Arctic Ocean, very low  $p\text{CO}_2$  ( $< 100$ – $150 \mu\text{atm}$ ) has been

observed co-located with under-ice phytoplankton blooms (Arrigo et al., 2012, 2014) and in the open waters of the Chukchi Sea (Bates et al., 2006). At the other end of the spectrum, high  $p\text{CO}_2$  values have been previously reported in the East Siberian Sea (e.g.  $> 1500 \mu\text{atm}$  in Tiksi Bay, Semiletov et al., 2007) and in the Chukchi Sea in surface waters (up to  $\sim 900 \mu\text{atm}$  in mixed layer water of Long Strait in the Chukchi Sea; this study) and bottom waters across the shelf (Bates et al., 2013).

In the one previous study of ice melt pond CO<sub>2</sub>–carbonate chemistry, Geilfus et al. (2012a) reported  $p\text{CO}_2$  values in the Amundsen Gulf in the Canadian Archipelago of  $\sim 79$  to  $348 \mu\text{atm}$  (Table 1) that were intermediate between the acidic and alkaline types observed in the Chukchi Sea during the ICESCAPE project.

There is a little more data from studies of melted sea-ice and sea-ice brines. In Fig. 7,  $\Omega_{\text{aragonite}}$  of ICESCAPE melt pond water is plotted against pH and  $p\text{CO}_2$  values. Superimposed on the figure are the ranges of  $p\text{CO}_2$  directly observed and/or pH and  $p\text{CO}_2$  computed from reported data of observed DIC and TA (while notable details are listed in Table 1, the reader is referred to the original literature also). The dashed boxes in the figure refer to the pH and  $p\text{CO}_2$  ranges of each study with colours denoting melted sea-ice (blue – fall/winter values; green – spring/summer values) and brines (blue fall values; purple – winter; red – spring/summer). The timing of sampling is likely an important factor to consider as ice melt water chemistry is likely influenced by sea-ice

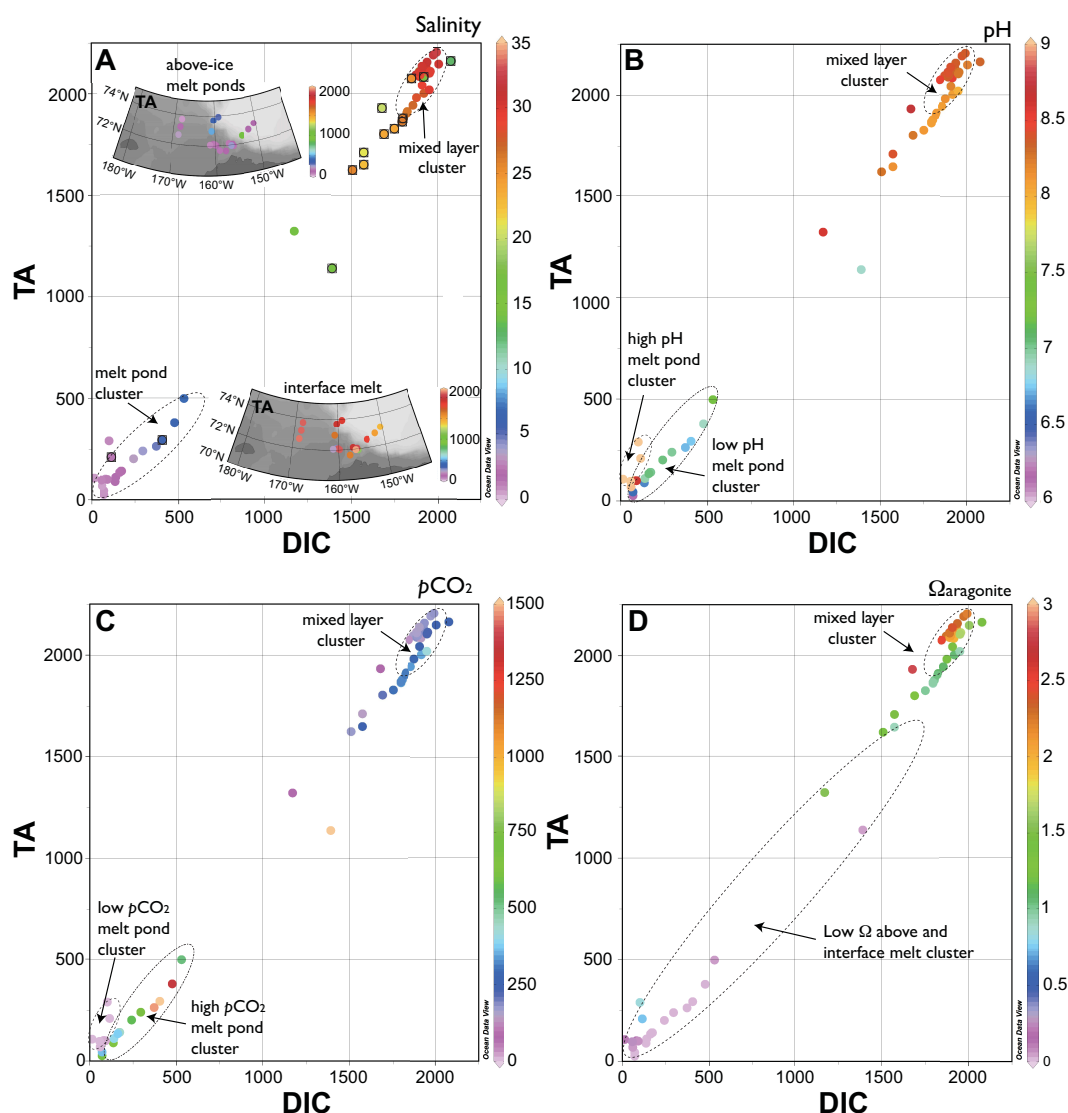


**Figure 5.** Scatter plots of CO<sub>2</sub>–carbonate chemistry for above-ice melt ponds, below-ice interface melt waters, and mixed-layer values beneath each ice station sampled on 2010 and 2011 ICESCAPE cruises. (a) DIC (μmol kg<sup>-1</sup>) versus total alkalinity (TA; μmol kg<sup>-1</sup>) with range of colour denoting salinity. Surface TA is shown for above-ice melt ponds and below-ice interface melt waters in the insets. The approximate chemical clustering of above-ice melt ponds, below-ice interface melt waters, and mixed-layer water is also shown. (b) DIC (μmol kg<sup>-1</sup>) versus total alkalinity (TA; μmol kg<sup>-1</sup>) with range of colour denoting pH. (c) DIC (μmol kg<sup>-1</sup>) versus total alkalinity (TA; μmol kg<sup>-1</sup>) with range of colour denoting pCO<sub>2</sub>. (d) DIC (μmol kg<sup>-1</sup>) versus total alkalinity (TA; μmol kg<sup>-1</sup>) with range of colour denoting Ω<sub>aragonite</sub> values.

and brine CO<sub>2</sub>–carbonate chemistry, and both the physical setting (e.g. ice temperature; sea-ice stratification; gas exchange) and variability of the biological community and biogeochemical processes within sea-ice.

During sea-ice advance/freeze-up, two highly contrasting scenarios have been reported. For example, very high pCO<sub>2</sub> values have been reported in sea-ice and brines (Matsuo and Miyake, 1966; Tison et al., 2002) while the calculated pCO<sub>2</sub> values at freeze-up were < 1 μatm in the Miller et al. (2011a) study (Table 1). In the latter study, the pH of brine water was highly alkaline (~ 12). In the wintertime, Miller et al.

(2011a) reported extremely high pCO<sub>2</sub> values for sea-ice and brines (ranging from 300 μatm to > 12 000 μatm, but mostly in the range of ~ 1000–2000 μatm) for both directly observed and computed pCO<sub>2</sub> in sea-ice of the Amundsen Gulf. In this same location, Miller et al. (2011b) also reported very high salinities in sea-ice (> 100), and DIC and TA values in the range of several thousand to > 10 000 μmoles kg<sup>-1</sup>).

In spring/summer sea-ice, other studies have shown smaller ranges of pCO<sub>2</sub> (~ < 1 to ~ 1500 μatm) and pH (~ 6.2 to 10.4) in comparison to the winter data of Miller et al. (2011a). As shown in Fig. 7, our ICESCAPE melt

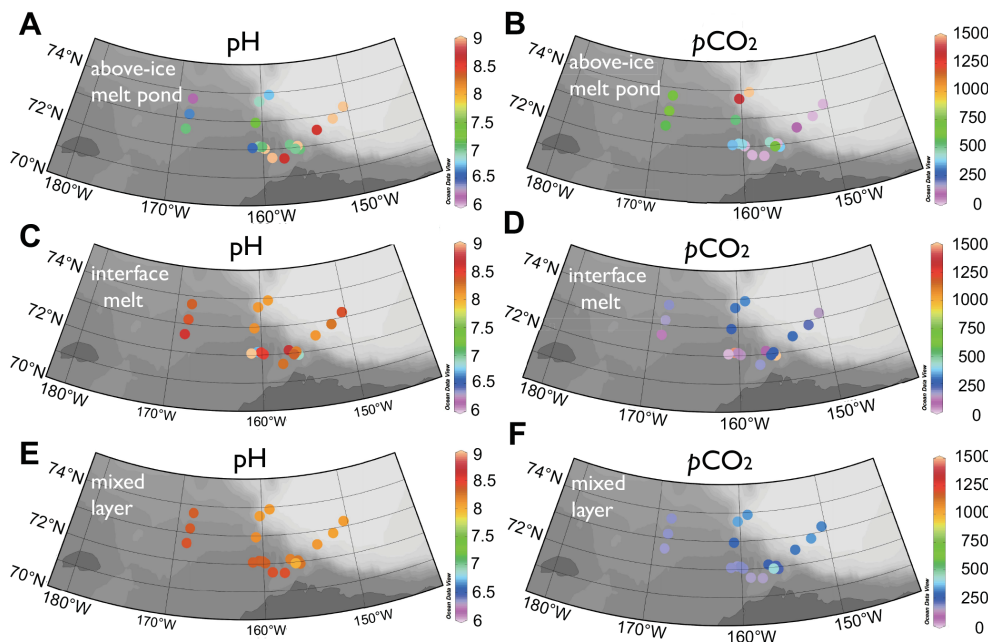


**Figure 6.** Surface maps of above-ice melt ponds, below-ice interface melt water, and mixed-layer values beneath each ice station sampled on 2010 and 2011 ICESCAPE cruises. (a) pH for above-ice melt ponds. (b)  $p\text{CO}_2$  ( $\mu\text{atm}$ ) for above-ice melt ponds. (c) pH for below-ice interface melt water. (d)  $p\text{CO}_2$  ( $\mu\text{atm}$ ) for below-ice interface melt water. (e) pH for mixed-layer values beneath each ice station. (f)  $p\text{CO}_2$  ( $\mu\text{atm}$ ).

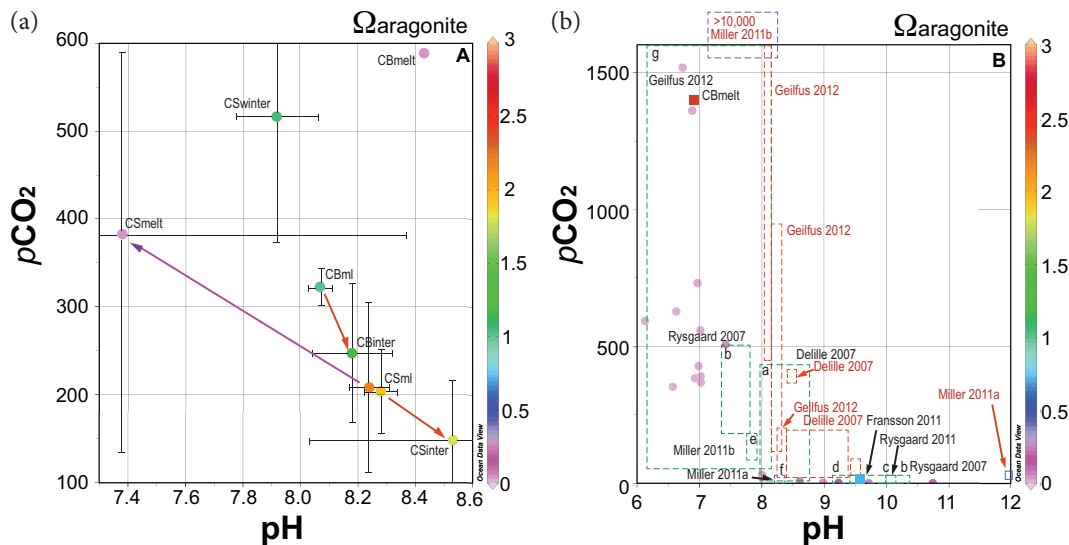


**Figure 7.** Scatter plot of above-ice and interface melt pond water pH against  $p\text{CO}_2$  ( $\mu\text{atm}$ ) with  $\Omega_{\text{aragonite}}$  values from the 2010 and 2011 ICESCAPE sea-ice stations in the western Arctic Ocean. Panel (a) shows mean and standard deviation for data collected on the Chukchi Sea shelf and Canada Basin. CSml, CSinter, CSmelt denote mean CO<sub>2</sub>–carbonate chemistry for the mixed-layer, interface and above-ice melt pond water for the Chukchi Sea (CS), respectively taken from Table 2. Winter water mean and standard deviation are also shown in the figure (CSwinter). CBml, CBinter, CBmelt denote mean CO<sub>2</sub>–carbonate chemistry for the mixed-layer, interface and above-ice melt pond water for the Canada Basin (CB), respectively taken from Table 2. In panel (b) ranges of CO<sub>2</sub>–carbonate chemistry from the ICESCAPE cruise are compared against the approximate ranges of  $p\text{CO}_2$  and pH directly observed or calculated from other studies (given in Table 1). The dashed boxes in the figure refer to the pH and  $p\text{CO}_2$  ranges of each study with colours denoting melted sea-ice (blue – fall/winter values; green – spring/summer values) and brines (blue fall values; purple – winter; red – spring/summer). Papers given in black or red text refer to melted sea-ice and brine studies, respectively.

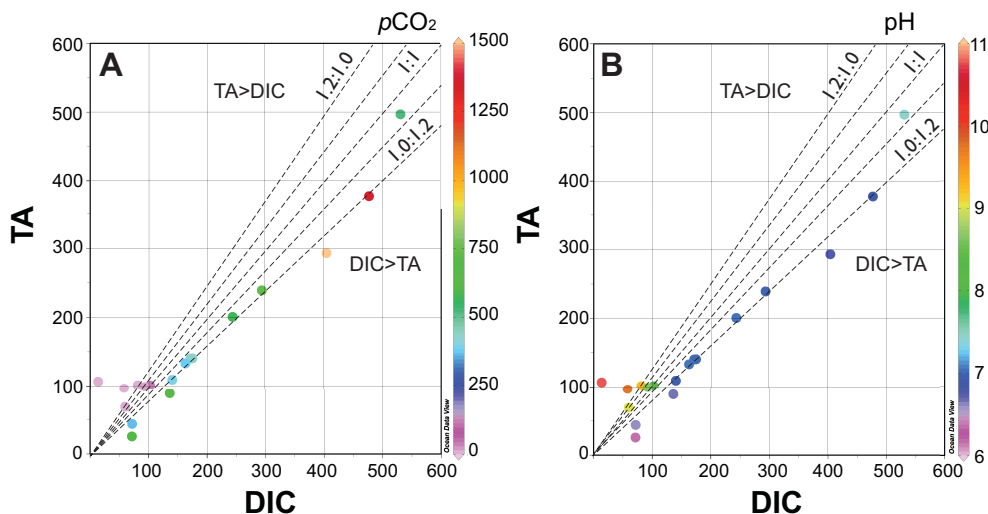


**Figure 8.** Scatter plots of TA and DIC against  $p\text{CO}_2$  –  $\mu\text{atm}$ , panel (a) and pH, panel (b) – for above-ice melt pond water sampled during the 2010 and 2011 ICESCAPE cruises in the western Arctic Ocean. The trend lines of TA : DIC ratios from 1.2 : 1.0 to 1.0 : 1.2 are shown.

pond data falls within the very large envelope of reported  $p\text{CO}_2$  and pH values, and encompasses both alkaline and acidic/neutral types of melted sea-ice and brines. In early-spring season studies, high  $p\text{CO}_2$  (> 500 to 1,500  $\mu\text{atm}$ ) has been reported (e.g. Geilfus et al., 2012a) with the highest  $p\text{CO}_2$  values in sea-ice of coldest temperature ( $\leq 10^\circ\text{C}$ ; Miller et al., 2011b; Geilfus et al., 2012a). During the spring-to-summer transition (before ice melt and breakup)  $p\text{CO}_2$  in melted sea-ice and brines seasonally decreases to lower values (e.g. Geilfus et al., 2012a), while pH, computed here, increases from a range of  $\sim 6.2$ – $8.2$  to  $> 9$  in some cases (pH estimated from the studies of Rysgaard et al., 2007; Fransson et al., 2011, Rysgaard et al., 2011 for example). Such seasonal changes in sea-ice chemistry likely reflect a combination of synergistic processes such as sea-ice warming (and brine loss), net autotrophy in sea-ice (e.g. Thomas and Dieckmann, 2010) and perhaps loss of  $\text{CO}_2$  from sea-ice by gas exchange and flux to the atmosphere (Delille et al., 2007).

In view of these previous reports of  $\text{CO}_2$ –carbonate chemistry observations in melted sea-ice and brines, the acidic/neutral and alkaline melt pond water types sampled in the Chukchi Sea and Canada Basin during the ICESCAPE expedition appear to fall within the  $p\text{CO}_2$  and pH ranges observed in brines and sea-ice (and one melt pond study; Geilfus et al., 2012a) in other polar regions.

#### 4.1.2 What are the possible causes of alkaline and acidic type melt pond waters?

As also noted above, melt water present in above-ice ponds in the western Arctic Ocean has a chemical composition that reflects the summed influence of several processes, including: (1) the initial composition of sea-ice after its formation and brine rejection during winter freeze-up, (2) any biogeochemical and physical modification during winter and (3) bio-

geochemical modification imparted by the biological community within sea-ice, mixing with seawater and influence of ice/air/seawater gas exchanges during the spring/early-summer melt.

Brine rejection during freeze-up can result in rejection of DIC and TA (Miller et al., 2011b) and export of inorganic carbon to bottom waters (e.g. Omar et al., 2005). Later, during the spring/summer transition, the net ecosystem metabolism (NEM) of sea-ice has considerable influence on  $\text{CO}_2$ –carbonate chemistry and includes: (1) net ecosystem production (i.e. NEP, balance and shift of autotrophic and heterotrophic activities in sea-ice, and (2) net ecosystem calcification (NEC) as sea-ice can be active regions of  $\text{CaCO}_3$  precipitation (e.g. ikaite formation, Papadimitriou et al., 2004; Dieckmann et al., 2008) or  $\text{CaCO}_3$  dissolution within the sea ice.

*Alkaline melt pond water.* As shown earlier, the first type of sea-ice source that contributes to above-ice melt pond water appears to be alkaline (i.e. low  $p\text{CO}_2$ /high pH; Fig. 7). In these alkaline melt pond waters, TA values are much greater than DIC (Fig. 8), and TA : DIC ratios have a mean of  $1.52 \pm 0.29:1.00$ , with lower  $p\text{CO}_2$  ( $\sim < 1$  to  $\sim 100 \mu\text{atm}$ ; Fig. 8a) and low pH ( $\sim 8.0$  to  $9.5$ ; Fig. 8b). These samples were primarily collected in the Canada Basin or at the edge of the Chukchi Sea shelf. In comparison, samples from the mixed layer beneath each ice station have a mean TA : DIC ratio of  $1.08 \pm 0.03 : 1.00$ , closer to typical surface waters of the North Pacific Ocean and western Arctic Ocean. Such chemistry of the alkaline melt water could result as a legacy of excess TA imparted during earlier brine rejection as shown by Miller et al. (2011b) in the Amundsen Gulf. However, it could also result from active generation of alkalinity in sea-ice, presumably as a result of  $\text{CaCO}_3$  dissolution. We have no direct evidence of earlier ikaite formation or its presence in

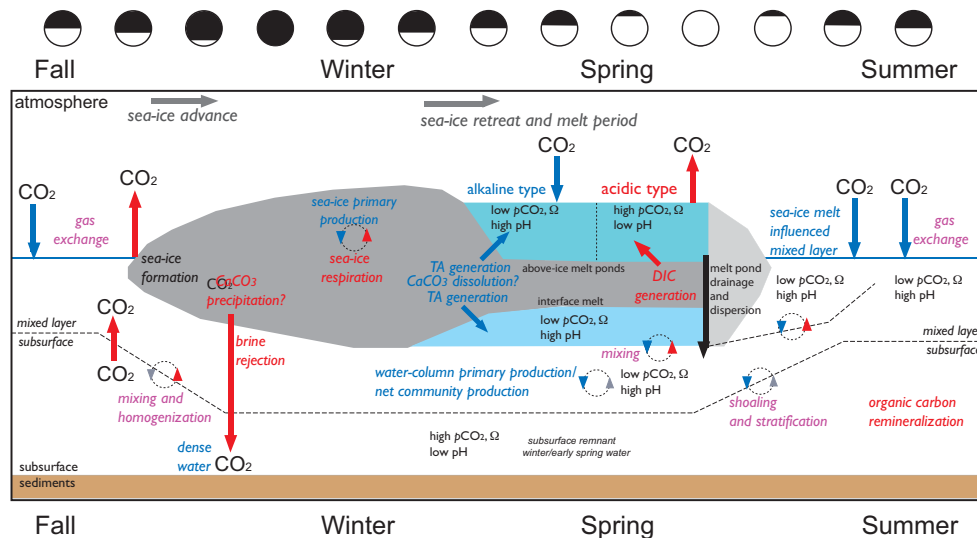


**Figure 9.** Seasonal schematic of processes impacting sea-ice and seawater CO<sub>2</sub>–carbonate chemistry in the western Arctic Ocean. The seasonal advance (freeze-up) and retreat (melting and breakup) of sea-ice is shown against approximate seasonal timing for both Arctic and Antarctic studies (both shown against season rather than month). Processes that can influence the decrease or increase of melt water or seawater  $p\text{CO}_2$  are shown in blue and red respectively. For example, photosynthesis and calcification reduces CO<sub>2</sub>. In the water column, generalized changes in mixed-layer depth and surface water stratification are shown. Also shown in the figure are idealized surface ice melt ponds and below-ice interface melt water. The above-ice melt pond is differentiated into the observed alkaline and acidic types observed during the ICESCAPE project in 2010 and 2011 in the Chukchi Sea.

sea-ice in the western Arctic, but CaCO<sub>3</sub> has been observed in sea-ice elsewhere in the Arctic (e.g. Papadimitriou et al., 2004; Dieckmann et al., 2008; Sogaard et al., 2013). In addition, an active coccolithophore community and CaCO<sub>3</sub> liths were observed in sea-ice at several of the ice stations during the 2011 ICESCAPE cruise (Balch et al., 2014).

**Acidic melt pond water.** The second type of sea-ice source that contributes to above-ice melt pond water was mildly acidic (high  $p\text{CO}_2$ /low pH) with very low TA : DIC ratios. In contrast to the alkaline type melt water, the acidic type had mean TA : DIC ratio of  $0.87 \pm 0.29 : 1.00$  (Table 2), with higher  $p\text{CO}_2$  ( $\sim 350$  to  $\sim 1500$   $\mu\text{atm}$ ; Fig. 8a) and low pH ( $\sim 6.1$  to  $7.5$ ; Fig. 8b). These melt pond waters were primarily sampled on the Chukchi Sea shelf. In such waters, DIC is greater than TA, a highly unusual condition when compared to most natural waters.

Unlike the alkaline type above-ice melt ponds, in the acidic type melt pond water, CO<sub>2</sub> equilibrium dictates that carbonate species were only present in the form of dissolved CO<sub>2</sub> [i.e. CO<sub>2</sub> + H<sub>2</sub>CO<sub>3</sub>] – and bicarbonate [HCO<sub>3</sub><sup>−</sup>] with negligible [CO<sub>3</sub><sup>2−</sup>] present. The mildly acidic pH (6.1 to 7.5) of several sea-ice melt waters sampled during the ICESCAPE expeditions (Fig. 8a) was thus unusual compared to typical seawater conditions. At these low pH levels, comparing with Bjerrum plots of [HCO<sub>3</sub><sup>−</sup>], [CO<sub>3</sub><sup>2−</sup>] and [CO<sub>2</sub>\*] against pH (see Butler, 1982; Zeebe and Wolfe-Gladrow, 2001), it is evident that [CO<sub>3</sub><sup>2−</sup>] was largely absent (or present in very low concentration) with [HCO<sub>3</sub><sup>−</sup>] and [CO<sub>2</sub>\*] being

the dominant carbonate species. Equilibrium thermodynamics of the CO<sub>2</sub>–carbonate system dictate that DIC is greater than TA in such waters. In several other studies of melted sea-ice and brines, samples with DIC values greater than TA have also been reported (e.g. Rysgaard et al., 2007; Miller et al., 2011a; Geilfus et al., 2012; Sogaard et al., 2013) concomitant with low pH ( $< 7.0$ ) and higher  $p\text{CO}_2$  (e.g.  $> 1,000$   $\mu\text{atm}$  and even as much as  $12,000$   $\mu\text{atm}$ ; Miller et al., 2011a). Our observation of TA : DIC ratios less than 1 in melt pond water from the ICESCAPE project appears to be a relatively common phenomenon in some sea-ice settings (e.g. brines, sea-ice and melt ponds) and infers strong influence of sea-ice metabolism and biogeochemical processes on CO<sub>2</sub>–carbonate chemistry.

#### 4.1.3 Can biological processes influence the type of melt pond water?

The ICESCAPE data suggest that highly variable sea-ice biology contributes to highly variable above-ice melt pond water CO<sub>2</sub>–carbonate chemistry. As shown in other sea-ice studies, the NEM of the sea-ice biological community is likely to influence melt pond chemistry (i.e. through balance of photosynthesis/net autotrophy versus respiration/net heterotrophy, Fig. 9). Our data also indicate that variability in the net balance of CaCO<sub>3</sub> production or dissolution (contributing either a deficit or excess of alkalinity, respectively) has a strong potential control on melt pond CO<sub>2</sub>–carbonate chemistry.

While there are few supporting data, there appears to be some difference in the metabolic status of sea-ice over the Chukchi Sea and Canada Basin. Sea-ice at the Canada Basin stations appear more likely to be net heterotrophic (source of CO<sub>2</sub> to the ice melt ponds) when compared to the Chukchi Sea shelf ice stations and other melt ponds reported in the literature (which may have been influenced by net autotrophy in the ice; Geilfus et al., 2012a). Chlorophyll *a* values in the alkaline, low *p*CO<sub>2</sub>/high pH melt ponds sampled over the Chukchi Sea shelf (stations 55–57, 90, 100) ranged from 0.05 to 0.30 μg L<sup>-1</sup>. In contrast, chlorophyll *a* biomass was much lower (0.01–0.03 μg L<sup>-1</sup>) in the acidic/neutral, high *p*CO<sub>2</sub>/low pH melt ponds present over the Canada Basin (stations 101, 127–129).

In the context of other studies of sea-ice settings (e.g. Fig. 7b), many of the above-ice ponds sampled during the ICESCAPE project appear not to have transitioned from “winter-early spring” high *p*CO<sub>2</sub>/low pH and Ω<sub>aragonite</sub> conditions (i.e. representing the low temperature/high *p*CO<sub>2</sub> state of early spring sea-ice; Miller et al., 2011b; Geilfus et al., 2012a) to low *p*CO<sub>2</sub>/high pH and Ω<sub>aragonite</sub> in response to net autotrophy and alkalinity generation within the sea-ice. Alternatively, since the melt water was sampled later in the season, the above-ice melt ponds may have transitioned from net autotrophy to net heterotrophy (thereby producing CO<sub>2</sub> which manifests in melt pond chemistry) in response to a later season increase in the microbial activity compared to autotrophic activity in sea-ice.

In the acidic type melt ponds of the Chukchi Sea and Canada Basin, where might the CO<sub>2</sub> originate from to produce high *p*CO<sub>2</sub>? Given the low DIC and TA values of melt pond water, relatively minor readjustment of CO<sub>2</sub>–carbonate equilibrium can result in high *p*CO<sub>2</sub> water. For comparison, the melt pond water concentration of [CO<sub>2</sub>] ranged from 20 to 45 μmol kg<sup>-1</sup> compared to a range of 10 to 18 μmol kg<sup>-1</sup> in the underlying mixed layer during the ICESCAPE project. For example, seasonal remineralization of dissolved organic carbon (DOC) produced earlier by sea-ice algae could provide sufficient CO<sub>2</sub> to generate acidic type melt pond water. In Greenland sea-ice, Sogaard et al. (2013) reported a rapid spring build-up of 40 to 60 μM of DOC in sea-ice that would be sufficient to generate high *p*CO<sub>2</sub> in melt water if this organic matter was remineralized to CO<sub>2</sub> during spring melt.

The high *p*CO<sub>2</sub> observed in melt ponds in the Canada Basin during the ICESCAPE project could also reflect the influence and legacy of wintertime high *p*CO<sub>2</sub> in brines and sea-ice (such as reported by Miller et al., 2011b). Alternatively, CaCO<sub>3</sub> production (e.g. through the formation of Ikaite), could also generate CO<sub>2</sub>, but Sogaard et al. (2013) reported low CaCO<sub>3</sub> concentrations (as particulate inorganic carbon) of 2 to 4 μmol L<sup>-1</sup>. While the latter rates of CaCO<sub>3</sub> production reported elsewhere appear insufficient to generate CO<sub>2</sub> in acidic type melt pond water, we do not have observations of melt pond DOC or PIC (Particulate Inorganic Carbon) to test such scenarios.

The other difference between above-ice melt ponds sampled in the western Arctic Ocean and other ice-covered regions is that the majority of them appear to be potentially transient sources of CO<sub>2</sub> to the atmosphere (Fig. 9). At least 60 % of the sampled above-ice melt pond waters had *p*CO<sub>2</sub> values higher than the atmosphere. This provides for an air–sea *p*CO<sub>2</sub> gradient that is favourable to the transfer of CO<sub>2</sub> to the atmosphere. In contrast, other sampled sea-ice melt ponds, with low *p*CO<sub>2</sub> relative to the atmosphere, appear to be potentially strong but transient sinks for atmospheric CO<sub>2</sub>, similar to observations reported elsewhere (e.g. Semiletov et al., 2004; Geilfus et al., 2012a). Our observations suggest that both scenarios, as shown in Fig. 9, exist for above-ice melt ponds in the western Arctic Ocean and that alkalinity variability and CaCO<sub>3</sub> precipitation/dissolution (i.e. increasing/decreasing *p*CO<sub>2</sub>) appear highly important for controlling CO<sub>2</sub> gas exchange between melt ponds and the atmosphere.

## 4.2 Interface melt CO<sub>2</sub>–carbonate chemistry

### 4.2.1 Interface water CO<sub>2</sub>–carbonate chemistry and comparisons to the contemporaneous mixed layer

As discussed earlier, interface water immediately between sea-ice and the mixed layer beneath were sampled at each sea-ice station. The majority of interface waters had salinity, TA and DIC values that were highly influenced by the mixed layer beneath, but a couple of samples had low salinity, TA and DIC values in the same range as the above-ice melt pond water (Fig. 10a). In general, the interface waters had lower salinity, TA, DIC and *p*CO<sub>2</sub>, and higher pH and Ω<sub>aragonite</sub> values compared to the co-located mixed layer beneath (mean values compared in Table 2). Similar to the above-ice melt pond water (Fig. 8), those interface waters with highest TA : DIC ratios tended to have the lowest *p*CO<sub>2</sub> (Fig. 10a) and highest pH values (Fig. 10b). As with the above-ice melt pond water, there was also geographic clustering with Chukchi Sea shelf interface waters having much lower *p*CO<sub>2</sub> and higher pH and Ω<sub>aragonite</sub> values compared to interface waters sampled out in the deep waters of the Canada Basin (Table 2). On the Chukchi Sea shelf, the mixed layer sampled at the ice stations had a mean *p*CO<sub>2</sub> (~ 204 ± 68 μatm; Fig. 10a; Table 2) similar to the mean shelf mixed-layer *p*CO<sub>2</sub> sampled from all of the ICESCAPE water column stations (~ 208 ± 131 μatm). These low mixed-layer *p*CO<sub>2</sub> values are comparable to historical summertime observations on the Chukchi Sea shelf over the last 10–15 years (e.g. Murata and Takizawa, 2003; Pipko et al., 2002; Bates, 2006; Bates et al., 2006, 2011). In contrast, the mixed-layer *p*CO<sub>2</sub> at the sea-ice stations in the deep Canada Basin were much higher at 315 ± 27 μatm (Fig. 10b; Table 2), similar to other observations of surface waters north of the Chukchi Sea shelf (e.g. Cai et al., 2010).

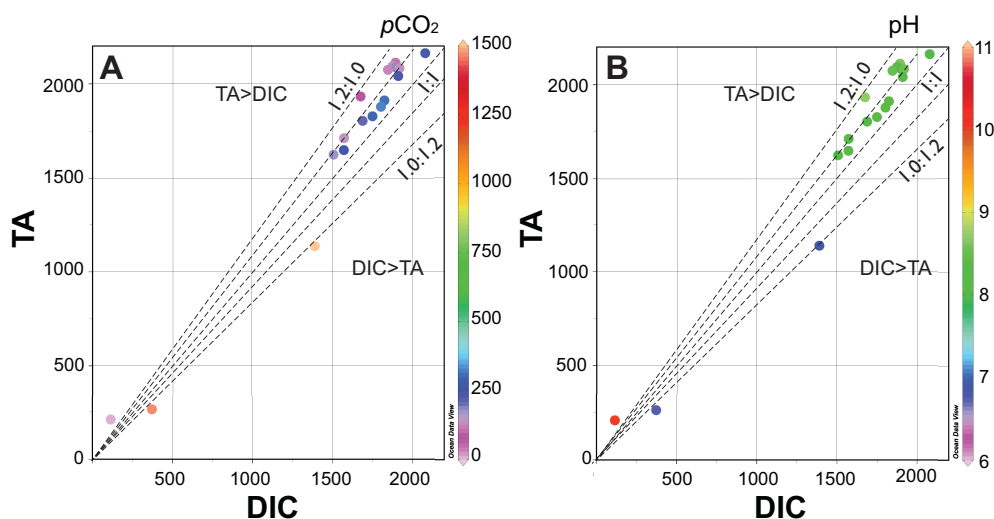


**Figure 10.** Scatter plots of TA and DIC against  $p\text{CO}_2$  ( $\mu\text{atm}$ ; panel a) and pH (panel b) for below-ice interface melt water sampled during the 2010 and 2011 ICESCAPE cruises in the western Arctic Ocean. The trend lines of TA : DIC ratios from 1.2 : 1.0 to 1.0 : 1.2 are shown.

#### 4.2.2 Can the CO<sub>2</sub>–carbonate chemistry sources for interface melt water be determined?

The chemistry of interface waters sampled during the ICESCAPE project offer clues to the nature of the under-ice melt contributions to the mixed layer. On the Chukchi Sea shelf, the interface waters of the shelf have lower  $p\text{CO}_2$ , and higher pH and  $\Omega_{\text{aragonite}}$  than the mean mixed-layer values (Fig. 7a; Table 2). Although the mean TA : DIC ratio of interface waters is similar to the mixed layer, the majority of samples have TA : DIC ratios of 1.13 : 1.00 to 1.17 : 1.00 (Fig. 10). These TA : DIC ratios are higher than the underlying mixed-layer seawater (1.09 : 1.00). Similar patterns occur in the Canada Basin with the mean  $n\text{TA} : n\text{DIC}$  ratio of the Canada Basin interface water difference being 1.058 : 1.00, and thus higher than the underlying mixed-layer  $n\text{TA} : n\text{DIC}$  ratio (1.04 : 1.00; Table 2).

Since interface waters are a composite mixture of seawater from the underlying mixed-layer and sea-ice melt, these data suggest that both TA and DIC, relative to mixed-layer conditions, were generated in sea-ice melt in order to produce the observed interface chemistry in the western Arctic (Fig. 11). A more nuanced suggestion from the data is that interface waters of the Chukchi Sea shelf and Canada Basin had excess TA relative to DIC (i.e. to produce TA : DIC ratios) compared to the underlying mixed layer. Since interface waters are a composite of melt water and mixed-layer water, the ICESCAPE data suggest that the melt water contribution to interface waters is alkaline with excess TA relative to DIC compared to mixed-layer waters of the region.

The underlying causes for the excess TA to DIC in the melt water contribution to interface waters cannot be quantified here, but a combination of processes at work can be invoked including: (1) a legacy of excess TA relative to DIC in

sea-ice resulting from freeze-up processes and winter physical and biogeochemical processes, (2) early summer NEP that is shifted to net respiration and production of CO<sub>2</sub>, and (3) generation of alkalinity in sea-ice through CaCO<sub>3</sub> dissolution. Irrespective of the causes, the sea-ice contributions to interface melt water results in the lowering of  $p\text{CO}_2$  and elevation of pH and  $\Omega$  values of interface waters compared to the underlying mixed layer.

#### 4.2.3 Assessing the potential impact of melt water on the underlying mixed-layer

The ice melt waters produced seasonally in the western Arctic Ocean have potential impacts on the CO<sub>2</sub>–carbonate chemistry of the mixed layer. Here, we use the differences in the mean hydrographic properties and CO<sub>2</sub>–carbonate chemistry of melted sea-ice, the mixed-layer and remnant winter water on the Chukchi Sea shelf (Table 2) as illustrative of the potential impact of sea-ice melt on the mixed layer. For example, the mixed-layer DIC and TA observed during the ICESCAPE project is an integrated sum of both winter water and melt water that has been contributed to by such processes as net ecosystem production and air–sea CO<sub>2</sub> gas exchange.

As Spall et al. (2014) have recently demonstrated, during both ICESCAPE cruises remnant winter water was present on the Chukchi Sea shelf below the mixed layer. The mean and range of salinity, temperature, inorganic nutrients and dissolved oxygen observed during the two ICESCAPE cruise from depths of 35 to 50 m (Table 2; from 70°N to the 200 m deep shelf break on the Chukchi Sea) had similar mean values and ranges to the winter water of Spall et al. (2014). For example, the remnant winter water, mixed layer (0–10 m) and melt pond at the sea-ice stations had mean salinities of 32.92, 30.08 and 1.85 (Table 2). If we assume that the shelf mixed-layer salinity is composed of both remnant winter water and

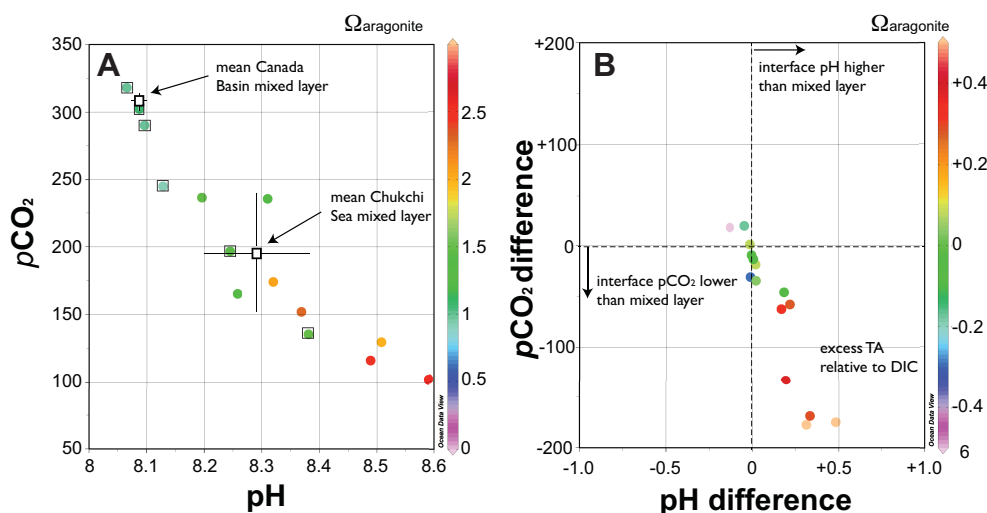


**Figure 11.** Scatter plots of interface melt water CO<sub>2</sub>–carbonate chemistry from the 2010 and 2011 ICESCAPE cruises in the western Arctic Ocean. Panel (a) denotes pH against pCO<sub>2</sub> (µatm) with range of colour denoting Ω<sub>aragonite</sub> values. The Canada Basin samples are denoted by symbols surrounded by square symbol. Panel (b) denotes the differences in pH against pCO<sub>2</sub> (µatm) and Ω<sub>aragonite</sub> values relative to the underlying mixed layer at each ice station.

ice melt dilution, by mass balance ice melt contributed ~9 % volume to mixed-layer waters. Cooper et al. (2014) also found that sea-ice melt contributed as much as 10 % to the mixed layer of the Chukchi Sea shelf using δ<sup>18</sup>O–salinity data collected during the ICESCAPE project.

In marine settings, seasonal changes in DIC, nutrients or dissolved oxygen can be used to provide time-integrated rates of net community production (NCP) that can be compared to short-term in situ <sup>14</sup>C-based rate estimates of net primary production. In the Chukchi Sea shelf, earlier studies have reported very high rates of primary production or NCP during the sea-ice free summertime period of 340–2850 mg C m<sup>-2</sup> d<sup>-1</sup> (e.g. Hameedi, 1978; Cota et al., 1996; Wheeler et al., 1996; Chen et al., 2002; Hill and Cota, 2005; Bates et al., 2005a; Mathis et al., 2008a) compared to other shelf environments in the Arctic Ocean. Annual rates of PP or NCP have been estimated at 35 to 364 g C m<sup>-2</sup> yr<sup>-1</sup> in the Chukchi Sea (Wheeler et al., 2005; Hill and Cota, 2005; Bates et al., 2005a). Recently, Arrigo et al., 2012 have shown high rates of primary production under sea-ice in the NW region of the Chukchi Sea during the ICESCAPE expedition.

In a mass balance sense, time-integrated NCP on the Chukchi Sea shelf can also be determined from geochemical changes in DIC from wintertime to the time of sampling (i.e. June to July). In simple terms, the change in DIC due to NCP (ΣDIC<sup>NCP</sup>) is equal to seasonal DIC changes that can be expressed as

$$\Sigma \text{DIC}^{\text{NCP}} = \Sigma \text{DIC}^{\text{WINTER}} - \Sigma \text{DIC}^{\text{MIXEDLAYER}} \quad (5)$$

The ΣDIC<sup>NCP</sup> term integrates changes in time (and space due to horizontal transport) and can be scaled to give a euphotic zone rate of NCP (with a euphotic zone depth of

30 m). However, as the ICESCAPE sea-ice data have suggested, sea-ice melt contribution is important and has to be taken into account in addition to air–sea CO<sub>2</sub> gas exchange contributions. Therefore, Eq. (5) is reformulated as

$$\begin{aligned} \Sigma \text{DIC}^{\text{NCP}} = & \left( \Sigma \text{DIC}^{\text{WINTER}} - \Sigma \text{DIC}^{\text{MIXEDLAYER}} \right) \\ & + \Sigma \text{DIC}^{\text{GASEX}} + \Sigma \text{DIC}^{\text{ICEMELT}}. \end{aligned} \quad (6)$$

Using Table 2 data and Eq. (5) only at first, mass balance yields a seasonal mean rate of NCP of 24.5 g C m<sup>-2</sup> period<sup>-1</sup> (i.e. from late winter to time of observations in early summer), integrating changes in DIC in a mixed layer of 30 m. The ΣDIC<sup>WINTER</sup> and ΣDIC<sup>MIXEDLAYER</sup> terms are mean observed values (Table 2). Here, the ΣDIC<sup>NCP</sup> term was converted from mol m<sup>-2</sup> to g C m<sup>-2</sup>, equivalent to the rate of NCP expressed as g C m<sup>-2</sup> period<sup>-1</sup>. Again, it should be noted that this is a generalized mean view of the above scenario and thus does not address the issue of temporal and spatial variability.

How potentially important are the gas flux and sea-ice melt terms since both should contribute DIC to the mixed layer to partially offset DIC drawdown due to NCP? If we include gas exchange (i.e. ΣDIC<sup>GASEX</sup>), the NCP term would increase by ~9.3 % to 26.9 g C m<sup>-2</sup> period<sup>-1</sup>. This gas flux term is computed using gas transfer coefficients of Wanninkhof (1992) and mean windspeed of 4 m s<sup>-1</sup> (mean for May to July in Chukchi Sea; Stegall and Zhang, 2012; Baule and Shulski, 2014) that yields a mean influx of ~4 mmoles CO<sub>2</sub> m<sup>-2</sup> d<sup>-1</sup> over a 50-day period (sea-ice free) and mixed-layer depth of 30 m. If the ΣDIC<sup>ICEMELT</sup> term is considered, the NCP increases by ~34.5 % from 24.5 g C m<sup>-2</sup> period<sup>-1</sup> to 33.0 g C m<sup>-2</sup> period<sup>-1</sup>. Including both gas flux and sea-ice

melt terms yields an NCP rate of 35.4 g C m<sup>-2</sup> period<sup>-1</sup>, 44.3 % higher than the scenario where gas exchange and sea-ice melt contributions are not considered.

The above scenario is illustrative, but clearly demonstrates the potential importance of considering the contribution of gas exchange and sea-ice melt to any estimates of NCP using DIC changes. If they were not included, then NCP rates determined from geochemical changes in DIC would be underestimated by at least a third.

### 4.3 Implications of melt pond and interface water CO<sub>2</sub>-carbonate chemistry for ocean acidification and air-sea CO<sub>2</sub> gas exchange

Findings from the ICESCAPE expeditions have implications for the present and future impact of ocean acidification and changing rates of air-sea CO<sub>2</sub> gas exchange in the Arctic Ocean. The melt pond waters exhibited two chemical types, alkaline and acidic, while the interface waters were predominantly alkaline. Melt pond  $\Omega_{\text{aragonite}}$  (and  $\Omega_{\text{calcite}}$ ) had saturation states less than 1 which infers that these waters are corrosive to CaCO<sub>3</sub> (these waters will also be corrosive for ikaite which has a higher solubility compared to aragonite; Papadimitriou et al., 2013). However, interface water contributes low  $p\text{CO}_2$ , and high pH and  $\Omega$  saturation states for CaCO<sub>3</sub> minerals to the mixed layer. Contemporaneously, in the Chukchi Sea, summertime net primary production in the euphotic zone tends to decrease  $p\text{CO}_2$  and increase pH and saturation states for CaCO<sub>3</sub> minerals such as calcite and aragonite in surface waters (e.g. Bates et al., 2009, 2013). In this scenario, both processes contribute to increasing pH and  $\Omega$  that should compensate each season and superimpose their impact on the long-term lowering of pH and in surface waters of the western Arctic due to anthropogenic CO<sub>2</sub> uptake (Bates et al., 2013) and Mackenzie river inputs to the region (Jutterstrom et al., 2009).

The contribution of sea-ice melt water to the balance of air-sea CO<sub>2</sub> sinks and sources in the Arctic Ocean is highly uncertain owing to the observed range of chemical melt pond types shown here or in previous studies (Geilfus et al., 2012a). The marginal sea-ice zone of the Arctic Ocean is presently about 12 million km<sup>2</sup> (i.e.  $\sim$  16 million km<sup>2</sup> sea-ice cover during the winter maxima which reduces to  $\sim$  4.5 to 6 million km<sup>2</sup> at its minima in the recent past). Sea-ice melt ponds are transient features in the Arctic Ocean (a couple of weeks to 1 month) and typically cover 20 to 50 % of the sea-ice surface area (Sejr et al., 2011). Although most of the melt ponds sampled had  $p\text{CO}_2$  values lower than the atmosphere, it is not possible to determine the net impact of melt ponds and interface waters on the rates of air-sea CO<sub>2</sub> gas exchange in the Arctic. Any assessment of the influence of above-ice and below-ice interface melt water chemistry on air-sea CO<sub>2</sub> sinks and sources thus requires further investigation to examine the seasonal CO<sub>2</sub> behaviour in many types of sea-ice melt water at different stages in the net metabolic condition

of the sea-ice, variability in CaCO<sub>3</sub> precipitation/dissolution processes, production of excess TA relative to DIC in melt water and determination of the relative proportion of alkaline versus acidic type sea-ice melt water across the region.

## 5 Conclusions

Observations of CO<sub>2</sub>-carbonate chemistry in above-ice melt ponds, below-ice interface melt water, and the water column across the western Arctic Ocean in the late spring/early summer of 2010 and 2011 were presented here. Contemporaneous examination of the CO<sub>2</sub>-carbonate chemistry of above-ice and below-ice melt waters and co-located, mixed-layer seawater has rarely been undertaken in sea-ice-covered oceans.

Our observations of CO<sub>2</sub>-carbonate chemistry at sea-ice stations in the western Arctic Ocean revealed highly variable melt pond water with both alkaline and acidic/neutral types. The  $p\text{CO}_2$  of melt pond water ranged from  $< 1$  to  $\sim 1,500 \mu\text{atm}$ , while pH ranged from mildly acidic (6.1 to 7.5) to alkaline (8.5 to 10.5). The melt pond water also had very low ( $< 0.1$ ) saturation states ( $\Omega$ ) for calcium carbonate (CaCO<sub>3</sub>) minerals such as aragonite ( $\Omega_{\text{aragonite}}$ ). This finding suggests that these above-ice melt ponds were potentially corrosive to CaCO<sub>3</sub> in the sea-ice melt. It is also likely that low  $\Omega$  ice melt pond water contributes to the low  $\Omega$  surface waters previously observed in the Canada Basin (Yamamoto-Kawai et al., 2005; Jutterstrom et al., 2009). In summary, above-ice melt pond water exhibited CO<sub>2</sub>-carbonate chemistry that corresponded to both scenarios discussed in the introduction and shown in Fig. 9.

In contrast to above-ice melt pond waters, the below-ice interface melt water sampled at the ice stations had lower  $p\text{CO}_2$  and higher pH /  $\Omega_{\text{aragonite}}$  than the co-located mixed layer beneath. Our analysis indicates that alkalinity is generated in sea-ice (at least excess TA to DIC) and contributes to below-ice melt water chemistry. This may be a legacy of wintertime physical and biological preconditioning of sea-ice but likely also results from active generation of alkalinity, from dissolution of CaCO<sub>3</sub> and net respiration in sea-ice. As shown in the conceptual summary of annual dynamics of CO<sub>2</sub>-carbonate chemistry (Fig. 9), the interface water has lower  $p\text{CO}_2$  (and higher pH and  $\Omega$ ) than the underlying mixed layer.

Above-ice melt ponds and below-ice melt waters are brief features observed in spring prior to breakup of sea-ice. While they are transient (4 to 6 weeks), sea-ice melt ponds can constitute greater than 50 % of the ice surface. In addition to their impact on albedo, heat, momentum and water exchanges in the high latitudes, our observations contribute to growing evidence that the impact of sea-ice on seawater CO<sub>2</sub>-carbonate chemistry is highly variable. This study, as in previous studies, confirms that further study of the dynamics and timing of all components of sea-ice chemistry (sea-ice, brines,

melt ponds) will be important for future assessments of the complex factors that influence the balance of CO<sub>2</sub> sinks and sources (and thereby ocean acidification) in the ice-covered high latitudes. With further warming and sea-ice loss predicted for the Arctic Ocean, for example, the presence of ice melt ponds and melt waters is likely to be greater in the expanded region of seasonal sea-ice retreat.

*Acknowledgements.* We would like to thank the captain and crew of the USCGC icebreaker *Healy*. We would like to especially thank K. Arrigo and many colleagues involved in the ICESCAPE project for their data contributions. Are Olsen and two anonymous reviewers are kindly thanked for their constructive reviews of the paper. N. R. Bates was supported by NASA award NNX10AG36G and NSF award PLR-1107457. K. E. Frey was supported by NASA award NNX10AH71G and NSF awards ARC-1107645 and ARC-1204044. J. T. Mathis was supported by NASA award NNX10AG36G and NSF award PLR-1107997.

Edited by: C. Heinze

## References

- Arctic Climate Impact Assessment (ACIA): Cambridge University Press, Cambridge, United Kingdom and New York, NY, USA, 2005.
- Arrigo, K. R., van Dijken, G., and Pabi, S.: Impact of a shrinking Arctic ice cover on marine primary production, *Geophys. Res. Lett.*, 35, L19603, doi:10.1029/2008GL035028, 2008.
- Arrigo, K. R., Perovich, D. K., Pickart, R. S., Brown, Z. W., van Dijken, G. L., Lowry, K. E., Mills, M. M., Palmer, M. A., Balch, W. M., Bates, N. R., Benitez-Nelson, C., Brownlee, E., Ehn, J. K., Frey, K. E., Garley, R., Laney, S. R., Mathis, J. T., Matsuoko, A., Mitchell, B. G., Moore, G. W. K., Ortega-Retuerta, E., Plasshenski, C. M., Reynolds, R. A., and Swift, J. H.: Massive phytoplankton blooms under Arctic sea-ice. *Science*, 336, 1408–1409, 2012.
- Balch, W. M., Bowler, B. C., Lubelczyk, L. C., and Stephens, M.: Aerial extent, composition, bio-optics and biogeochemistry of a massive under-ice algal bloom in the Arctic, *Deep-Sea Res. II*, 105, 42–58, 2014.
- Bates, N. R.: Air-sea CO<sub>2</sub> fluxes and the continental shelf pump of carbon in the Chukchi Sea adjacent to the Arctic Ocean. *Journal of Geophysical Research (Oceans)*, 111, C10013, doi:10.129/2005JC003083, 2006.
- Bates, N. R. and Mathis, J. T.: The Arctic Ocean marine carbon cycle: evaluation of air-sea CO<sub>2</sub> exchanges, ocean acidification impacts and potential feedbacks, *Biogeosciences*, 6, 2433–2459, doi:10.5194/bg-6-2433-2009, 2009.
- Bates, N. R., Moran, S. B., Hansell, D. A., and Mathis, J. T.: An increasing CO<sub>2</sub> sink in the Arctic Ocean due to sea-ice loss?, *Geophys. Res. Lett.*, 33, L23609, doi:10.1029/2006GL027028, 2006.
- Bates, N. R., Orchowska, M. I., Garley, R., and Mathis, J. T.: Present day vulnerability of the western Arctic seafloor to seasonal ocean acidification, *Biogeosciences*, 10, 5281–5309, doi:10.5194/bg/bg-10-5281-2013, 2013.
- Baule, W. J. and Shulski, M. D.: Climatology and trends of wind speed in the Beaufort/Chukchi Sea coastal region from 1979 to 2009, *Internat. J. Climatol.*, 34, 2819–2833, 2014.
- Brewer, P. G. and Goldman, J. C.: Alkalinity changes generated by phytoplankton growth, *Limnol. Oceanogr.*, 21, 108–117, 1976.
- Butler, J. N.: Carbon dioxide equilibria and their applications, Addison-Wesley Publications, 255 pp., 1982.
- Cai, W.-J., Chen, L., Chen, B., Gao, Z., Lee, S. H., Chen, J., Pierrot, D., Sullivan, K., Wang, Y., Hu, X., Huang, W.-J., Zhang, Y., Xu, S., Murata, A., Grebmeier, J. M., Jones, E. P., and Zhang, H.: Decrease in the CO<sub>2</sub> uptake capacity in an ice-free Arctic Ocean basin, *Science*, 329, 556, doi:10.1126/science.1189338, 2010.
- Carmack, E. and Wassman, P.: Food webs and physical-biological coupling on pan-Arctic shelves: Unifying concepts and comprehensive perspectives, *Prog. Oceanogr.*, 71, 446–477, 2006.
- Cavalieri, D., Parkinson, C., Gloersen, P., and Zwally, H. J.: updated yearly. Sea Ice Concentrations from Nimbus-7 SMMR and DMSP SSM/I-SSMIS Passive Microwave Data, [2009, 2010, 2011 monthly climatology], Boulder, Colorado USA, National Snow and Ice Data Center, 1996.
- Cooper, L. W., Frey, K. E., Wood, C. L., and Grebmeier, J. M.: Melted sea ice in an under-ice phytoplankton bloom in the Chukchi Sea, *Ocean Sciences Meeting, Hawaii, February 2014*, 2014.
- Cota, G. F., Pomeroy, L. R., Harrison, W. G., Jones, E. P., Peters, F., Sheldon, W. M., and Weingartner, T. R.: Nutrients, primary production and microbial heterotrophy in the southeastern Chukchi Sea: Arctic summer nutrient depletion and heterotrophy, *Mar. Ecol. Prog. Ser.*, 135, 247–258, 1996.
- Delille, B., Jourdain, B., Borges, A. V., Tison, J. L., and Delille, D.: Biogas (CO<sub>2</sub>, O<sub>2</sub>, dimethylsulfide) dynamics in spring Antarctic fast ice. *Limnol. Oceanogr.*, 52, 1367–1379, 2007.
- Dickson, A. G. and Millero, F. J.: A Comparison of the Equilibrium Constants for the dissociation of carbonic acid in seawater media, *Deep Sea Res. Part A*, 34, 1733–1743, 1987.
- Dickson, A. G., Sabine, C. L., and Christian J. R.: Guide to best practices for ocean CO<sub>2</sub> measurements, PICES Special Publication 3, IOCCP Report no. 8, 2007.
- Dieckmann, G. S. and Hellmer, H. H.: The importance of sea ice: An overview, in: *Sea Ice, an Introduction to its Physics, Chemistry, Biol. Geol.*, 2nd ed., edited by: Thomas, D. N. and Dieckmann, G. S., 1–22, Blackwell Sci., Oxford, UK, 2010.
- Dieckmann, G. S., Nehrke, G., Papadimitriou, S., Gottlicher, J., Steininger, R., Kennedy, H., Wolf-Gladrow, D., and Thomas, D. N.: Calcium carbonate as ikaite crystals in Antarctic sea ice, *Geophys. Res. Lett.*, 35, L08501, doi:10.1029/2008GL033540, 2008.
- Fransson, A., Chierici, M., Yager, P. L., and Smith, W. O.: Antarctic sea ice carbon dioxide system and controls, *J. Geophys. Res.-Oc.*, 116, C12035, doi:10.1029/2010JC006844, 2011.
- Geilfus, N. X., Carnat, G., Papakyriakou, T., Tison, J. L., Else, B., Thomas, H., Shadwick, E., and Delille, B.: Dynamics of pCO<sub>2</sub> and related air-ice CO<sub>2</sub> fluxes in the Arctic coastal zone (Amundsen Gulf, Beaufort Sea), *J. Geophys. Res.*, 117, C00G10, doi:10.1029/2011JC007118, 2012a.
- Geilfus, N. X., Delille, B., Verbeke, V., and Tison, J. L.: Towards a method for high vertical resolution measurements of the partial pressure of CO<sub>2</sub> within bulk sea ice, *J. Glaciol.*, 58, 287–300, 2012b.

- Gosselin, M., Legendre, L., Therriault, J. C., Demers, S., and Rochet, M.: Physical control of the horizontal patchiness of sea-ice microalgae, *Mar. Ecol. Prog. Ser.*, 29, 289–298, 1986.
- Hill, V. J. and Cota, G. F.: Spatial patterns of primary production in the Chukchi Sea in the spring and summer of 2002, *Deep Sea Res. Part II*, 52, 3344–3354, 2005.
- Jutterstrom, S. and Anderson, L. G.: Uptake of CO<sub>2</sub> by the Arctic Ocean in a changing climate, *Mar. Chem.*, 122, 96–104, 2010.
- Legendre, L., Ackley, S. F., Dieckmann, G. S., Gulliksen, B., Horner, R., Hoshiai, T., Melnikov, I. A., Reeburgh, W. S., Spindler, M., and Sullivan, C. W.: Ecology of sea ice biota. 2. Global significance, *Polar Biol.*, 12, 429–444, 1992.
- Maslanik, J.A., Drobo, S., Fowler C., Emery, W., and Barry R., 2007. On the Arctic climate paradox and the continuing role of atmospheric circulation in affecting sea ice conditions.
- Mathis, J. T. and Questel, J. M.: The impacts of primary production and respiration on the marine carbonate system in the Western Arctic: Implications for CO<sub>2</sub> fluxes and ocean acidification, *Cont. Shelf Res.*, 67, 42–51, 2013.
- Mathis, J. T., Bates, N. R., Hansell, D. A., and Babila, T.: Interannual variability of net community production over the northeast Chukchi Sea shelf. *Deep-Sea Res., II*, 56, 17, 1213–1222, 2009.
- Matsuo, S. and Miyake, Y.: Gas composition in ice samples from Antarctica, *J. Geophys. Res.*, 71, 5235–5241, 1966.
- McGuire, A. D., Chapin, F. S., Walsh, J. E., and Wirth, C.: Integrated regional changes in arctic climate feedbacks: implications for the global climate system, *Ann. Rev. Environ. Resour.*, 31, 61–91, 2006.
- McGuire, A. D., Anderson, L., Christensen, T. R., Dallimore, S., Guo, L. D., Hayes, D., Heimann, M., Macdonald, R., and Roulet, N.: Sensitivity of the carbon cycle in the Arctic to climate change (Review), *Ecol. Monogr.*, 79, 523–555, 2009.
- Mehrbach, C., Culberson, C. H., Hawley, J. E., and Pytkowicz, R. M.: Measurement of the apparent dissociation constants of carbonic acid in seawater at atmospheric pressure: *Limnol. Oceanogr.*, 18, 897–907, 1973.
- Miller, L. A., Carnat, G., Else, B. G. T., Sutherland, N., and Papkyriakou, T. N.: Carbonate system evolution at the Arctic Ocean surface during autumn freeze up, *J. Geophys. Res.-Oc.*, 116, C00G04, doi:10.1029/2011JC007143, 2011a.
- Miller, L. A., Papkyriakou, T. N., Collins, R. E., Deming, J. W., Ehn, J. K., Macdonald, R. W., Mucci, A., Owens, O., Raudsepp, M., and Sutherland, N.: Carbon dynamics in sea ice: A winter flux time series, *J. Geophys. Res.-Oc.*, 116, C02028, doi:10.1029/2009JC006058, 2011b.
- Murata, A. and Takizawa, T.: Summertime CO<sub>2</sub> sinks in shelf and slope waters of the western Arctic Ocean, *Continent. Shelf Res.*, 23, 753–776, 2003.
- Omar, A., Johannessen, T., Bellerby, R. G. J., Olsen, A., Anderson, L. G., and Kivimäe, C.: Sea ice and brine formation in Storfjorden: Implications for the Arctic wintertime air-sea CO<sub>2</sub> flux, in: *The Nordic Seas: An Integrated Perspective: Oceanography, Climatology, Biogeochemistry, and Modeling*, edited by: Drange, H., Dokken, T., Furevik, T., Gerdes, R., and Berger, W., *Geoph. Monogr.*, 158, 177–187, 2005.
- Pabi, S., van Dijken, G. L., and Arrigo, K. R.: Primary production in the Arctic Ocean, 1998–2006, *J. Geophys. Res.*, 113, C08005, doi:10.1029/2007JC004578, 2008.
- Papadimitriou, S., Kennedy, H., Kattner, G., Dieckmann, G. S., and Thomas, D. N.: Experimental evidence for carbonate precipitation and CO<sub>2</sub> degassing during sea ice formation, *Geochimica et Cosmochimica Acta*, 68, 1749–1761, 2004.
- Papadimitriou, S., Kennedy, H. J., Kennedy, P., and Thomas, D. N.: Ikaite solubility in seawater-derived brines at 1 atm and temperatures to 265 K, *Geochimica et Cosmochimica Acta*, 109, 241–253, 2013.
- Pickart, R. S., Spall, M. A., Schulze, L. M., Moore, G. W., and Brugler, E.: Role of shelfbreak upwelling on primary productivity in the Beaufort and Chukchi Seas. *Ocean Sciences Meeting, Hawaii*, Feb. 2014 (Abstract ID:13371), 2014.
- Pipko I. I., Semiletov I. P., Tishchenko P. Y., Pugach S. P., and Christensen J. P.: Carbonate chemistry dynamics in Bering Strait and the Chukchi Sea, *Prog. Oceanogr.*, 55, 77–94, 2002.
- Robbins, L. L. Hansen, M. E., Kleypas, J. A., and Meylan, S. C.: CO<sub>2</sub>calc: a user-friendly seawater carbon calculator for Windows, Max OS X, and iOS (iPhone), US Geological Survey Open-File Report, 2010–1280, 1–17, 2010.
- Rysgaard, S., Glud, R. N., Sejr, M. K., Bendtsen, J., and Christensen, P. B.: Inorganic carbon transport during sea ice growth and decay: A carbon pump in polar seas, *J. Geophys. Res.*, 112, C03016, doi:10.1029/2006JC003572, 2007.
- Rysgaard, S., Bedtsen, J., Delille, B., Dieckmann, G. S., Glud, R. N., Kennedy, H., Mortensen, J., Papadimitriou, S., Thomas, D. N., and Tison, J. L.: Sea ice contribution to the air-sea CO<sub>2</sub> exchange in the Arctic and Southern Oceans. *Tellus, Series B, Chem. Phys. Meteorol.*, 63, 823–830, 2011.
- Sabine, C. L., and Tanhua, T.: Estimation of anthropogenic CO<sub>2</sub> inventories in the ocean, *Ann. Rev. Mar. Sci.*, 2, 175–198, 2010.
- Schlitzer, R.: Ocean Data View, <http://odv.awi.de> (last accessed: 5 May 2012), 2011.
- Sejr, M. K., Krause-Jensen, D., Rysgaard, S., Sorensen, L. L., Christensen, P. B., and Glud, R. N.: Air-sea flux of CO<sub>2</sub> in Arctic coastal waters influenced by glacial melt water and sea ice. *Tellus, Series B, Chem. Phys. Meteorol.*, 63, 815–822, 2011.
- Semiletov, I. P., Makshtas, A., Akasofu, S. I., and Andreas, E. L.: Atmospheric CO<sub>2</sub> balance: The role of Arctic sea ice, *Geophys. Res. Lett.*, 31, L05121, doi:10.1029/2003GL017996, 2004.
- Semiletov, I., Pipko, I., Repina, I., and Shakhova, N. E.: Carbonate chemistry dynamics and carbon dioxide fluxes across the atmosphere-ice-water interfaces in the Arctic Ocean: Pacific sector of the Arctic, *J. Mar. Syst.*, 66, 204–226, 2007.
- Serreze, M. C. and Francis, J. A.: The Arctic amplification debate, *Clim. Change*, 76, 241–264, 2006.
- Sogaard, D. H., Thomas, D. N., Rysgaard, S., Glud, R. N., Norman, L., Kaartakallio, H., Juul-Pedersen, T., and Geilfus, N. X.: The relative contributions of biological and abiotic processes to carbon dynamics in subarctic sea-ice, *Polar Biol.*, 36, 1761–1777, 2013.
- Stegall, S. T. and Zhang, J.: Wind field climatology, changes, and extremes in the Chukchi–Beaufort Seas and Alaska North Slope during 1979–2009, *J. Climate*, 25, 8075–8089, 2012.
- Steinacher, M., Joos, F., Frölicher, T. L., Plattner, G.-K., and Doney, S. C.: Imminent ocean acidification in the Arctic projected with the NCAR global coupled carbon cycle-climate model, *Biogeosciences*, 6, 515–533, doi:10.5194/bg-6-515-2009, 2009.

- Stumm, W., and Morgan, J. J.: Aquatic Chemistry. An Introduction Emphasizing Chemical Equilibria in Natural Waters, John Wiley and Sons, New York, 780 pp., 1981.
- Takahashi, T., Sutherland, S. C., Wanninkhof, R., Sweeney, C., Feely, R. A., Chipman, D. W., Hales, B., Friederich, G. E., Chavez, F. P., Watson, A. J., Bakker, D. C. E., Schuster, U., Metzl, N., Yoshikawa-Inoue, H., Olafsson, J., Arnarson, T. S., Tilbrook, B., Johannessen, T., Olsen, A., Bellerby, R. J., de Baar, H. J. W., Nojiri, Y., Wong, C. S., Delille, B., and Bates, N. R.: Climatological mean and decadal change in surface ocean  $p\text{CO}_2$ , and net sea-air CO<sub>2</sub> flux over the global oceans, *Deep-Sea Res. II*, 56, 554–577, 2009.
- Tanhua, T., Bates, N. R., and Kortzinger, A.: The Marine Carbon Cycle and Ocean Anthropogenic CO<sub>2</sub> Inventories, in: *Ocean Circulation and Climate*, 103, Elsevier Press, 2013.
- Thomas, D. N., and Dieckmann, G. S. (Eds.): *Sea Ice*, 2nd Edn., 402 pp., Blackwell Sci., Oxford, UK, 2010.
- Tison, J.-L., Haas, C., Gowing, M. M., Sleewaegen, S., and Bernard, A.: Tank study of physico-chemical controls on gas content and composition during growth of young sea ice, *J. Glaciol.*, 48, 177–191, 2002.
- Wheeler, P. A., Gosselin, M., Sherr, E., Thibault, D., Kirchman, D. L., Benner, R., and Whitley, T. E.: Active cycling of organic carbon in the central Arctic Ocean, *Nature*, 380, 697–699, 1996.
- Zeebe, R. E. and Wolf-Gladrow, D.: *CO<sub>2</sub> in Seawater: Equilibrium, Kinetics, Isotopes*. Elsevier, Amsterdam, 2001.
- Zemmelink, H. J., Delille, B., Tison, J. L., Hints, E. J., Houghton, L., and Dacey, J. W. H.: CO<sub>2</sub> deposition over the multi-year ice of the western Weddell Sea, *Geophys. Res. Lett.*, 33, L13606, doi:10.1029/2006GL026320, 2006.